

Electronic Supplementary Information

Novel near infra-red fluorescent pH sensors based on
1-aminoperylene bisimides covalently grafted to
poly(acryloylmorpholine)

Daniel Aigner, Sergey M Borisov, Peter Petritsch and Ingo Klimant

Institute of Analytical Chemistry and Food Chemistry
Graz University of Technology
Graz, Austria.

Further result details

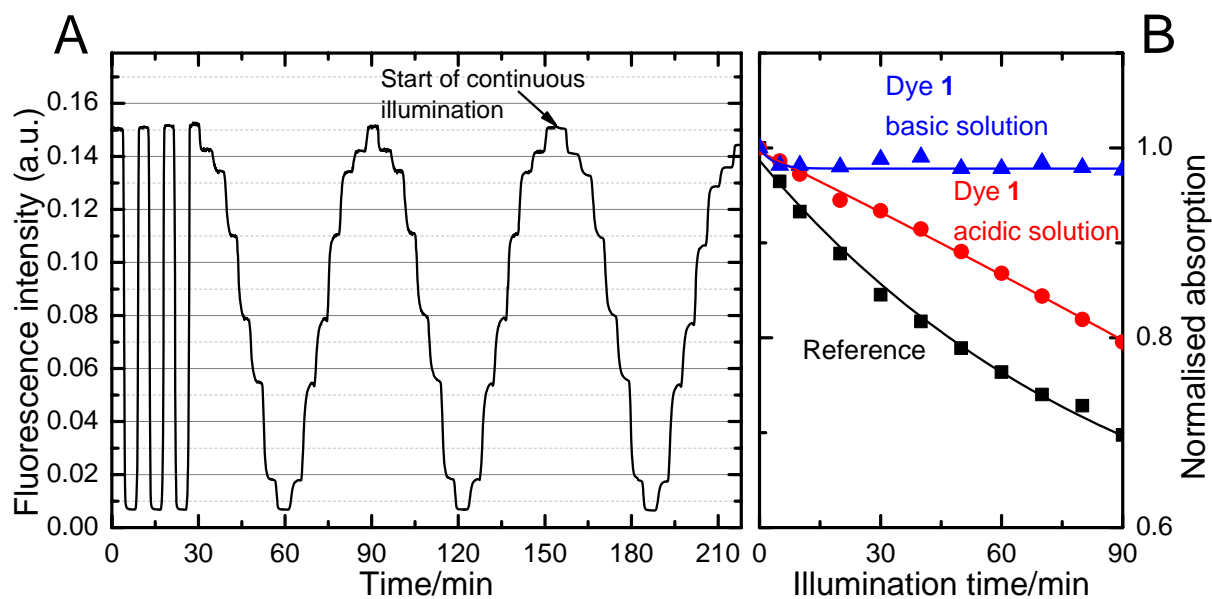


Figure ESI1: **A**: Performance of **3** (0.2 % (w/w)), covalently coupled to a cross-linked poly(acryloylmorpholine) layer (thickness 20 μm) in long-term measurement and under varying illumination conditions – the LED used for excitation is switched to continuous illumination (until then illumination time was 14% of the total measurement time). > 1 h of continuous illumination causes an error of < 0.1 pH units, when calculated over the calibration curve. Note that in practical applications continuous illumination is not necessary and an interrogation time of 30 ms is typically sufficient to obtain a measurement point. Thus 1 h of continuous illumination equals about 100,000 measurement points which enables a long measurement time (days or weeks, depending on the application). **B**: Photodegradation profiles of **1** and SNARF decyl ester as a reference in *N,N*-dimethylformamide (acidic: 0.1% V/V trifluoroacetic acid; basic: 0.1% V/V ethyldiisopropylamine) when illuminated with a high-power LED array (645 nm). Absorption was observed in the respective maxima, *i.e.* 630 nm for acidic **1**, 670 nm for basic **1**, 657 nm for the reference. Initial absorptions were 1.1 at 645 nm.

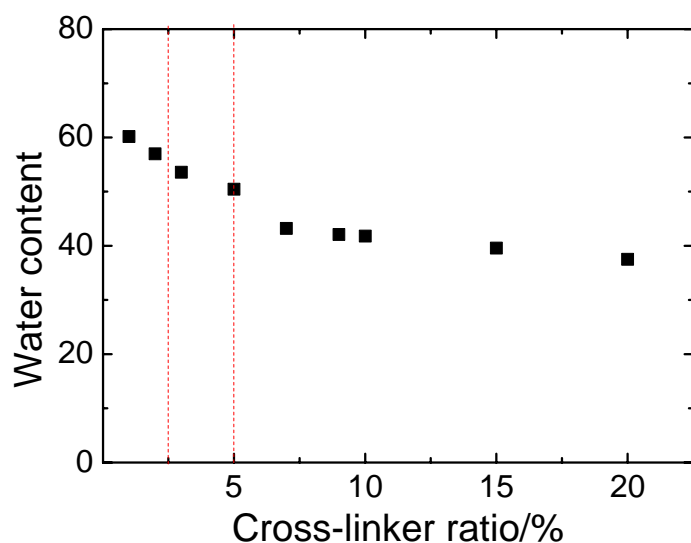


Figure ESI2: Water content of poly(acryloylmorpholine) in the swollen state as a function of the cross-linker (polyethylene glycol diacrylate) ratio used (% w/w with respect to the total monomer weight). Water content was determined gravimetrically. The cross-linking degrees used in sensors in this work are 5 % for the intensity based sensor and 2.5 % for the dually lifetime referenced sensor (dashed lines).

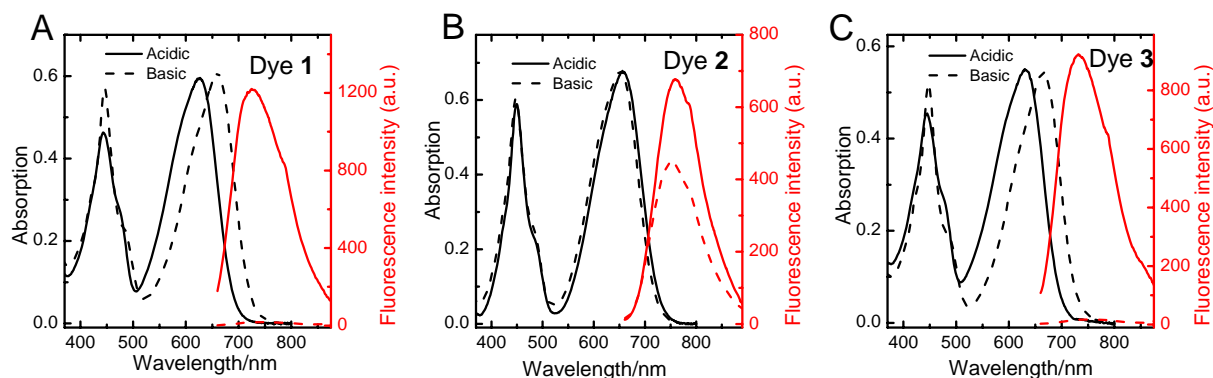


Figure ESI3: Spectral properties of **1** (A), **2** (B) and **3** (C) in tetrahydrofuran/water 9:1 (V/V). Solutions were acidified with HCl (10 mM) and made basic with ethyldiisopropylamine (ratio 0.1 % V/V). Concentrations were 30 μ M for measuring absorption and 3 μ M for fluorescence. Fluorescence was excited in the respective isosbestic points.

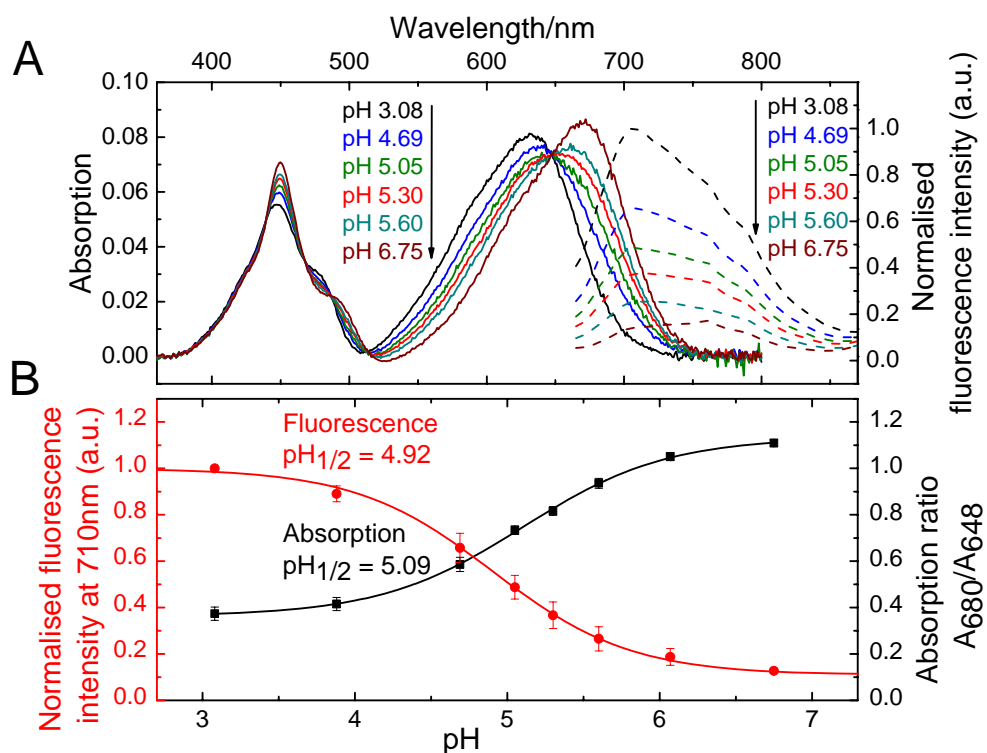


Figure ESI4: **A**: Absorption (solid) and fluorescence spectra (dashed) of **1** in D4 hydrogel (dye content 0.5 % (w/w), layer thickness 7 μm) at different pH (aqueous buffer, ionic strength 100 mM). Fluorescence was excited in the isosbestic point (648 nm). **B**: Corresponding calibration curves. $\text{pH}_{1/2}$ is the value at which half of the pH induced signal change is effective.

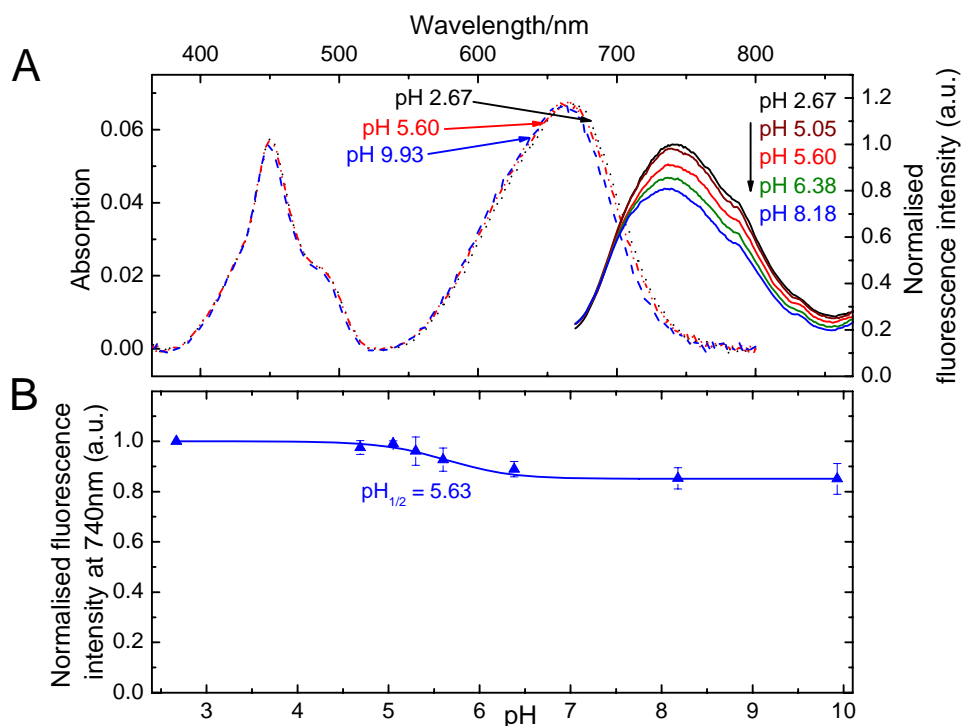


Figure ESI5: **A**: Absorption (dashed) and fluorescence spectra (solid) of **2** in D4 hydrogel (dye content 0.5 % (w/w), layer thickness 7 μm) at different pH (aqueous buffer, ionic strength 100 mM). **B**: Corresponding calibration curve based on fluorescence emission in the maximum. $\text{pH}_{1/2}$ is the value at which half of the pH induced signal change is effective. Absorption is virtually independent on pH, calibration is not shown.

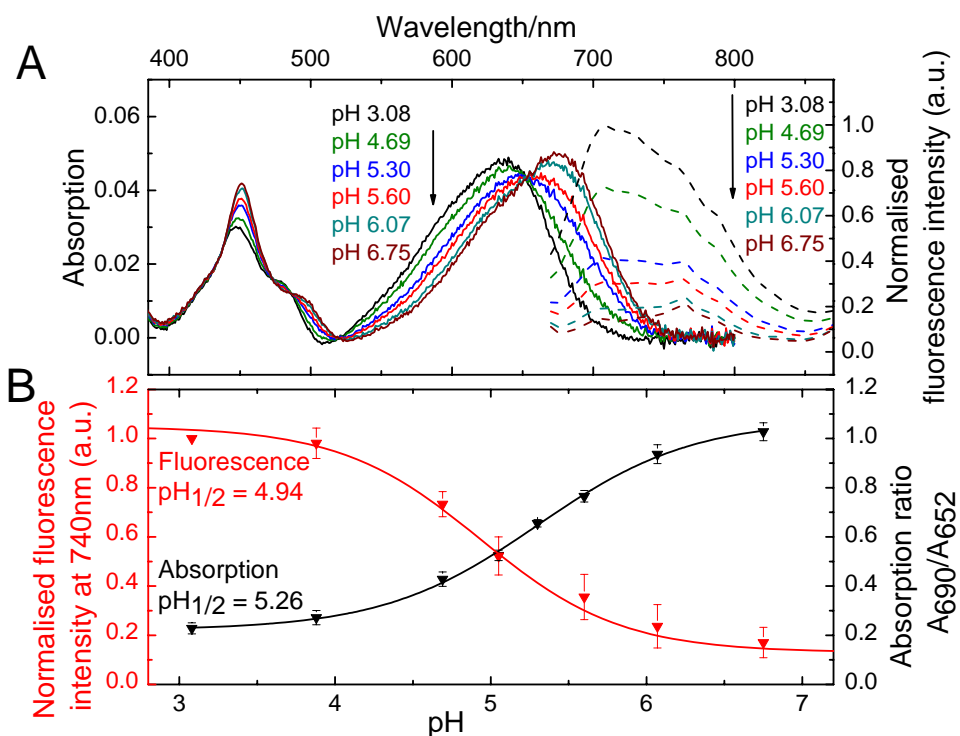


Figure ESI6: **A**: Absorption (solid) and fluorescence spectra (dashed) of **3** in D4 hydrogel (dye content 0.5 % (w/w), layer thickness 7 μm) at different pH (aqueous buffer, ionic strength 100 mM). Fluorescence was excited in the isosbestic point (652 nm). **B**: Corresponding calibration curves. $\text{pH}_{1/2}$ is the value at which half of the pH induced signal change is effective.

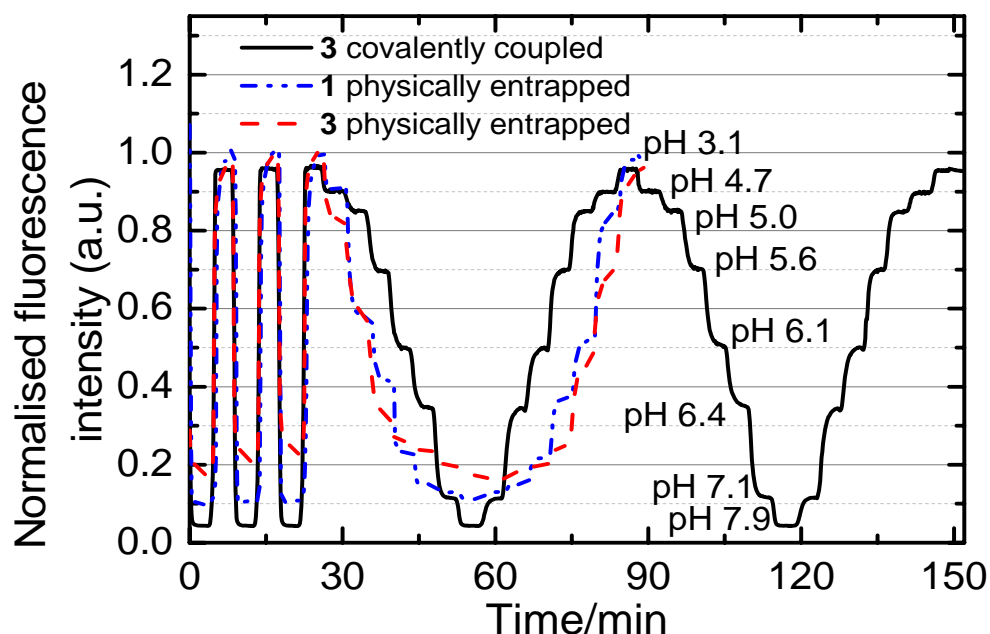


Figure ESI7: Dynamic response of the pH sensor with covalently grafted **3** (layer as specified below fig. ESI1) in long-term measurement, compared to D4 hydrogel sensors where **3** and **1** are physically entrapped (dye content 0.5% w/w, layer thickness 7 μm).

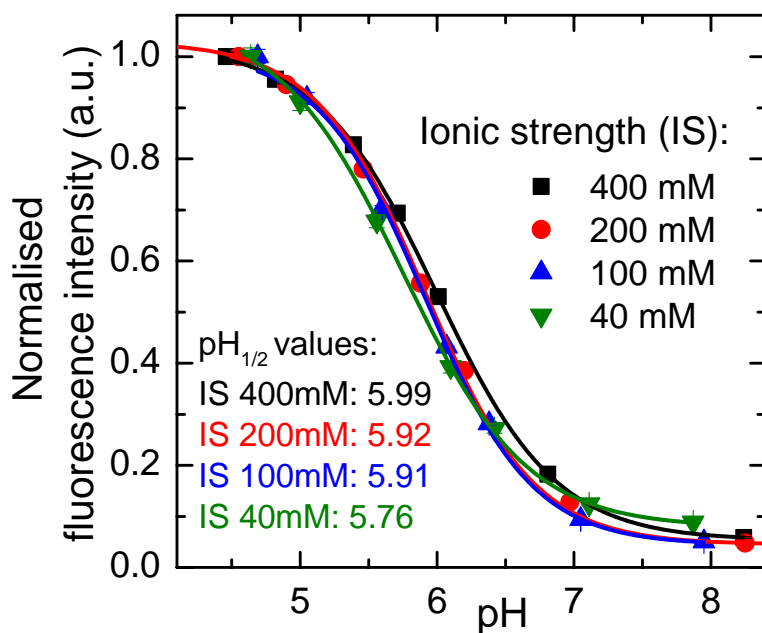


Figure ESI8: Calibration curves of **3** (layer as specified below fig. ESI1), measured at different ionic strengths. pH_{1/2} is the pH at which half of the pH induced signal change is effective.

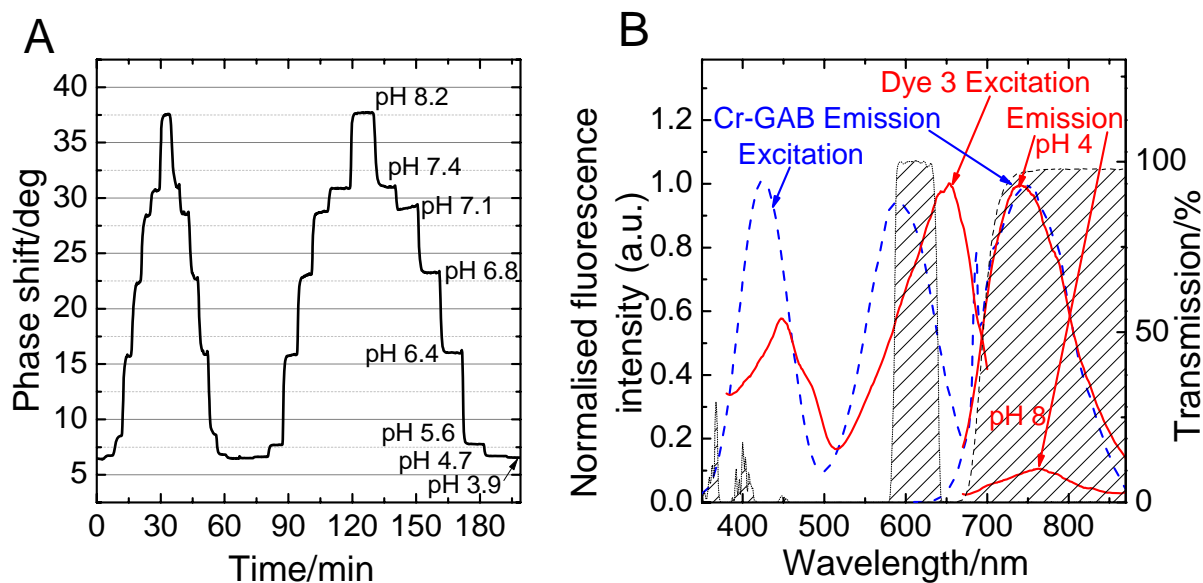


Figure ESI9: **A**: Dynamic response of a dually lifetime referenced (DLR) sensor, *i.e.* **3** (0.1 % w/w), covalently coupled to a cross-linked poly(acryloylmorpholine) layer (thickness 20 μm) containing phosphorescent Cr³⁺-doped gadolinium aluminium borate (Cr-GAB; 25 % w/w; molar Cr³⁺ content 2.5 % with respect to Al³⁺) as reference material. **B**: Spectral properties of the components of the DLR sensor. The transmissions of the excitation filter (585 - 640 nm) and emission filter (> 695 nm) are visualised by striped areas.

Materials and Methods

Materials

1,6,7,12-Tetrachloro-*N,N'*-di(2,6-diisopropylphenyl)perylene-3,4:9,10-tetracarboxylic bisimide (**4a**) and 1,6,7,12-tetrachloro-*N*-(2,6-diisopropylphenyl)-*N'*-((2-dibutylamino)ethyl)perylene-3,4:9,10-tetracarboxylic bisimide (**4c**) were synthesised from 1,6,7,12-tetrachloroperylene-3,4:9,10-tetracarboxylic bisanhydride (purchased from Beijing Wenhaiyang Industry and Trading Co.Ltd, <http://china.zhaoteng.com>) as reported elsewhere¹. 1-Methyl-2-pyrrolidone was from TCI Europe (<http://www.tcichemicals.com>). Solvents used for work-up and purification (synthesis grade) and for LCMS (HPLC-MS grade) as well as NaCl, buffer salts and microscope slides were supplied by Carl Roth (www.roth.de). Deuterated solvents were obtained from eurisotop (www.eurisotop.com). Silica gel (0.040-0.063 mm) was purchased from Acros (www.fishersci.com), polyurethane hydrogel D4 from CardioTech (www.cardiotech-inc.com). Chrome(III)-doped gadolinium aluminium borate phosphors were prepared in analogy to a procedure described elsewhere.² All other chemicals were from Sigma-Aldrich (www.sigmaaldrich.com). Poly(ethylene glycol terephthalate) support (Mylar[®]) was from Goodfellow (www.goodfellow.com).

Methods

Absorption measurements were performed on a Cary 50 UV-VIS spectrophotometre from Varian (www.varianinc.com). Fluorescence spectra were recorded on a Hitachi F-7000 spectrofluorimetre (www.hitachi.com). Relative fluorescence quantum yields were determined at 25 °C using Nile Blue ($\Phi_F = 0.27$ in ethanol)³ as a standard. NMR spectra were recorded on a 300 MHz instrument (Bruker; coupling constants *J* will be stated in Hz) with TMS as a standard. MALDI-TOF mass spectra were recorded on a Micromass TofSpec 2E. The spectra were taken in reflectron mode at an accelerating voltage of +20 kV. For LCMS measurements, a Nucleodor 100-5 μm C18ec reversed phase column (Macherey Nagel; 130 x 8mm) was used; mobile phases were water/acetic acid 1000:1 (V/V) and acetonitrile (gradients are stated in tables ESI1 and ESI2). A HP/agilent G1315A diode array detector and a Shimadzu LSMS-2020 mass detector (www.shimadzu.de; electrospray ionisation) were employed.

Sensor response curves and pH calibration curves were measured in a home-made stainless steel flow-through cell, pumping buffer with a flow rate of 1 ml min⁻¹ (except for the pH calibration curves of the sensors in D4 hydrogel which were measured with the spectrofluorimetre, sensors were incubated in a cuvette filled with buffer solution for 1min prior to measurement). Cell temperature was kept constant at 25 °C. The sensors were interrogated with a two-phase lock-in amplifier (SR830, Stanford Research Inc., www.thinksrs.com) equipped with a red LED (λ_{max} 629 nm) from Roithner (www.roithner-laser.com), a 620/50 nm bandpass filter from Edmund optics (www.edmundoptics.de) at the excitation side and a 695 nm long-pass filter (Schott, www.schott.com) before the PMT tube (H5701-02, Hamamatsu, www.sales.hamamatsu.com). The modulation frequency of 160 Hz was used for intensity measurement, while dually lifetime referenced sensors were measured employing a modulation frequency of 2.5 KHz.

The pH of the phosphate and phosphate-citrate buffer solutions was controlled by a digital pH meter (InoLab pH/ion, WTW GmbH & Co. KG, www.wtw.com) calibrated at 25 °C with standard buffers of pH 7.0 and 4.0 (WTW GmbH & Co. KG, www.wtw.com). The buffers were adjusted to a constant ionic strength of 100 mM using sodium chloride as the background electrolyte.

Photostability measurements were performed by irradiating the samples with the light of a 645 nm high-power 10 W LED array (www.led-tech.de) focused through a lens purchased from Edmund optics. The photodegradation profiles were obtained by monitoring the absorption spectra.

Calibration

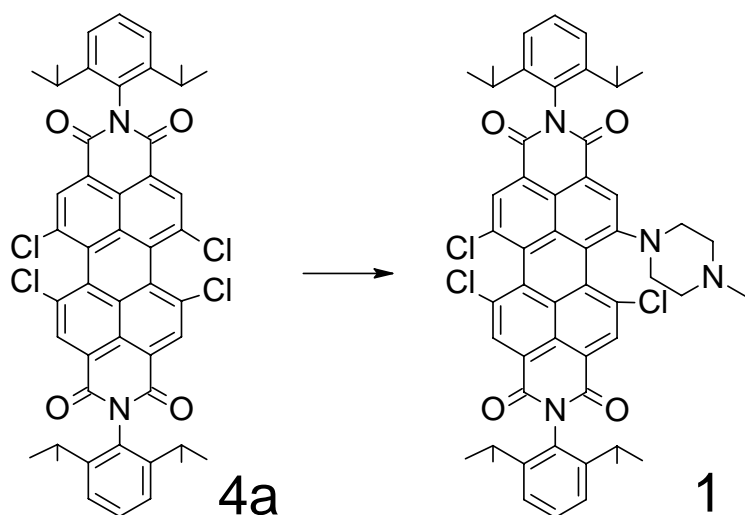
The following sigmoidal function was used for sensor calibration:

$$I = \frac{A_{\text{min}} - A_{\text{max}}}{1 + e^{(pH - pK_a)/dx}} + A_{\text{max}}, \quad (\text{equation 1})$$

where I - fluorescence intensity, A_{max} , A_{min} , and dx are numerical coefficients.

Syntheses

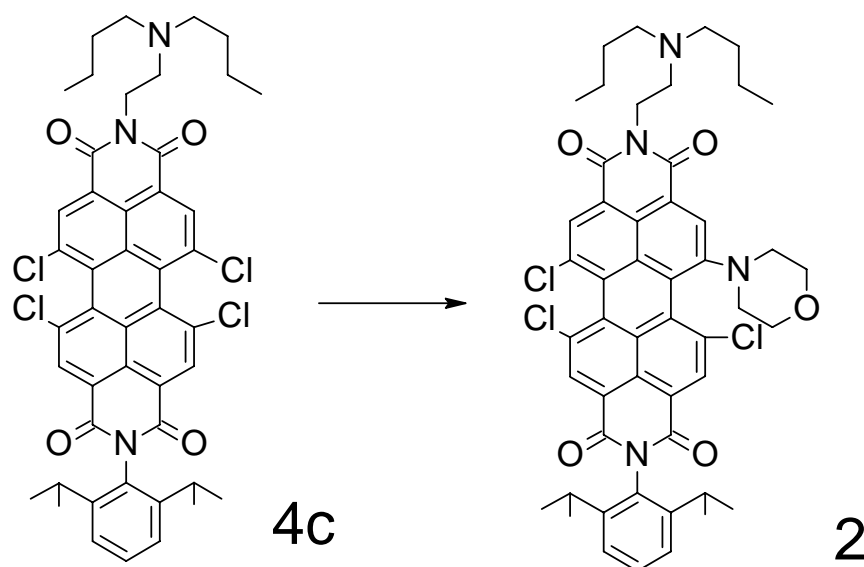
N,N'-di(2,6-diisopropylphenyl)-1-(4-methyl-1-piperazinyl)-6,7,12-trichloroerylene-3,4:9,10-tetracarboxylic bisimide (**1**)



Scheme ESI1: Preparation of **1**.

4a (250 mg, 0.29 mmol) was added to a mixture of *N*-methylpiperazine (1.2 ml, 10.8 mmol) and 1-methyl-2-pyrrolidone (1.2 ml) at 40 °C. The mixture was stirred for 60 min, 0.1 M aqueous HCl/saturated aqueous NaCl 1:1 (V/V) (100 ml) was added, the green precipitate was washed with water/saturated aqueous NaHCO₃ 9:1 (V/V) (2 * 50 ml) and water (2 * 50 ml) and dried. Column chromatography with silica gel (40 – 63 μm) as the stationary and CH₂Cl₂:MeOH 70:1 (V/V) as the mobile phase afforded **1** (158 mg, 60 %). NMR spectroscopy: δ_{H} (300 MHz, CDCl₃) 8.75 (2 H, d, ArH (Core)), 8.59 (2 H, d, ArH (Core)), 7.53 (2 H, t, *J* 7.8, ArH), 7.38 (4 H, d, *J* 7.8, ArH); 4.29 (2 H, br s, NCH₂), 2.87-3.10 (2 H, m, NCH₂), 2.70-2.87 (4 H, m, ArCH), 2.48-2.70 (2 H, m, NCH₂), 2.38 (3 H, s, NCH₃), 2.25-2.34 (1 H, br s, NCH₂), 1.96-2.15 (1 H, br s, NCH₂), 1.21 (24 H, m, ArCHCH₃). δ_{C} (300 MHz, CDCl₃) 163.6, 163.1, 162.9, 162.8 (C=O); 151.8, 145.9 (2 C), 145.7 (2 C), 135.6, 133.8 (2 C), 133.4, 133.3, 133.2, 132.3, 130.5, 130.4, 130.0 (2 C), 129.8, 129.7, 128.3, 124.6, 124.3-124.4 (4 C), 124.0, 123.8, 123.4, 122.1, 120.8, 119.6 (aromatic); 55.1, 54.6, 52.3, 47.5, 45.9 (NCH₂); 29.3-29.5 (multiple C, ArCH); 24.1-24.4 (multiple C, ArCHCH₃). MALDI-TOF *m/z* 911.2974 found, 911.2897 calculated.

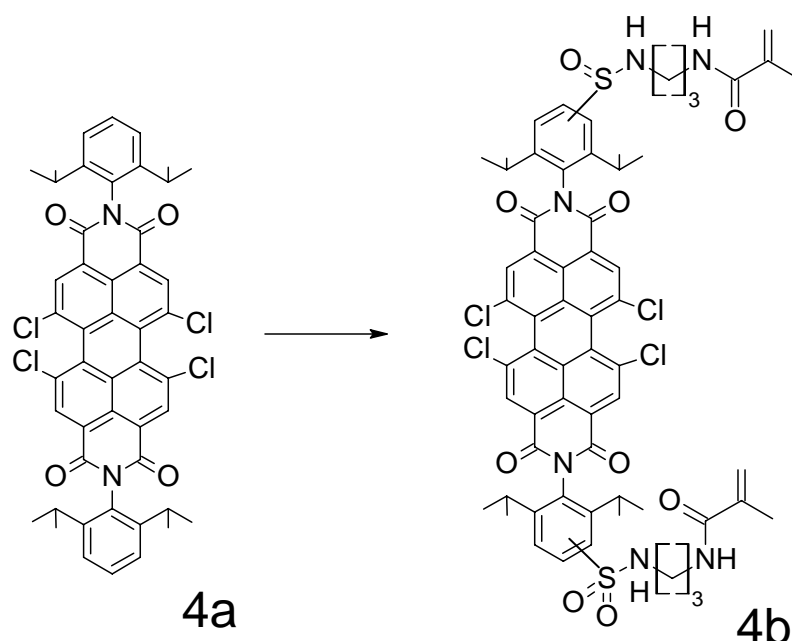
N-(2-(*N,N*-dibutylamino)ethyl)-*N'*-(2,6-diisopropylphenyl)-1-(4-morpholinyl)-6,7,12-trichloroperylene-3,4:9,10-tetracarboxylic bisimide (**2**)



Scheme ESI2: Preparation of **2**.

4c (65 mg, 0.077 mmol) was added to a mixture of morpholine (0.65 ml, 7.4 mmol) and 1-methyl-2-pyrrolidone (0.65 ml) at 40 °C. The mixture was stirred for 90 min, 0.1 M aqueous HCl/saturated aqueous NaCl 1:1 (V/V) (20 ml) was added and the green precipitate was washed with water/saturated aqueous NaHCO₃ 9:1 (V/V) (2 * 25 ml) and water (2 * 25 ml) and dried. The crude product was purified by column chromatography with silica gel (40 – 63 μm) as the stationary and CH₂Cl₂:MeOH (starting material was eluted with a ratio of 200:1 (V/V), product with 50:1) as the mobile phase to yield **2** (40 mg, 58 %). NMR spectroscopy: δ_H (300 MHz, CDCl₃) 8.70 (2 H, d, ArH (Core)), 8.52 ppm (2 H, d, ArH (Core)), 7.51 (1 H, t, *J* 7.8, ArH), 7.37 (2 H, d, *J* 7.8, ArH), 4.40 (2 H, br s, (CO)₂NCH₂), 4.18-4.28 (1 H, m, NCH₂CH₂O), 4.04-4.18 (2 H, m, NCH₂CH₂O (1 H) and OCH₂ (1 H)), 3.82-4.00 (1 H, m, OCH₂), 3.50-3.69 (1 H, m, OCH₂), 3.28-3.43 (1 H, m, OCH₂), 2.18-3.28 (9 H, m, (CO)₂NCH₂CH₂N (2 H) and NCH₂ (4 H) and NCH₂CH₂O (1 H) and ArCH (2 H)), 2.06-2.18 (1 H, m, NCH₂CH₂O), 1.38-1.69 (4 H, br s, NCH₂CH₂), 1.30-1.38 (4 H, m, NCH₂CH₂CH₂), 1.11-1.27 (12 H, q, *J* 5.9, ArCHCH₃), 0.92 (6 H, t, NCH₂CH₂CH₂CH₃). δ_C (300 MHz, CDCl₃) 163.5, 162.9, 162.7 (2C) (C=O); 151.5, 145.7, 145.5, 135.4, 133.6, 133.1, 132.7, 132.6, 131.9, 130.3, 130.1 (2 C), 129.8, 129.7, 129.5, 128.1, 124.2, 124.1, 123.9, 123.7, 123.2, 123.1, 120.6, 119.8 (aromatic); 66.9, 66.0 (OCH₂); 53.9 (broad), 52.7, 50.8 (broad), 47.8 (NCH₂); 29.2 (ArCH); 24.0 (ArCHCH₃); 20.4, 13.9 (Alkyl). MALDI-TOF *m/z* 893.3066 found, 893.3004 calculated.

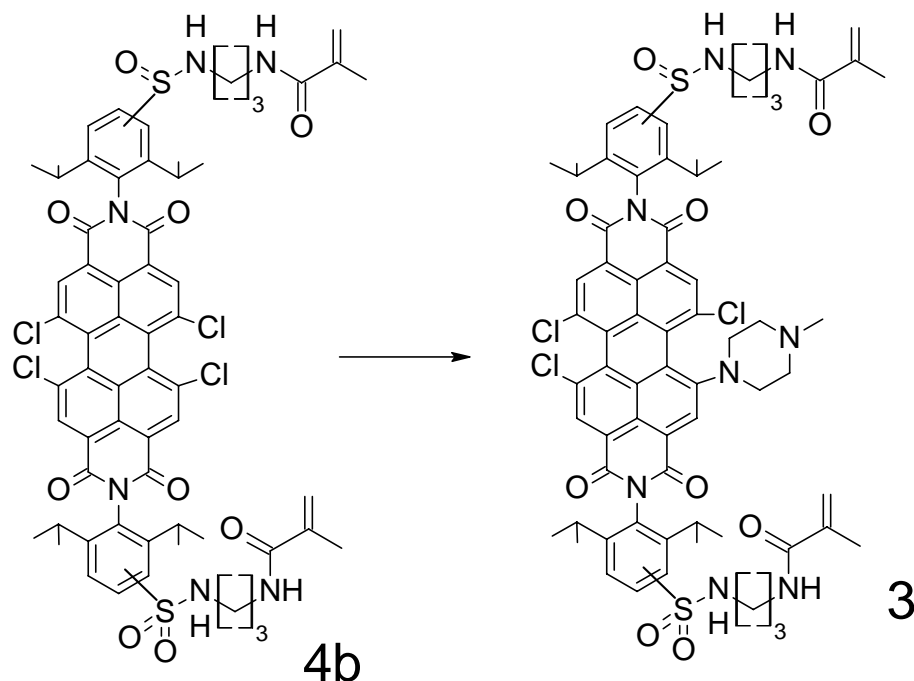
N-3-([*N*-(3-(methacryloylamino)propyl)amino]sulfonyl)-2,6-diisopropylphenyl)-*N'*-(4-([*N*-(3-(methacryloylamino)propyl)amino]sulfonyl)-2,6-diisopropylphenyl)-1,6,7,12-tetrachloro-*p*erylene-3,4:9,10-tetracarboxylic bisimide (**4b**)



Scheme ESI3: Preparation of **4b**.

4a (400 mg, 0.47 mmol) was heated to 60 °C in chlorosulfonic acid (4 ml) for 3 h. The reaction mixture was allowed to cool to RT and added dropwise onto crushed ice. The orange precipitate was transferred into a funnel, washed with ice water until neutral and dried applying a rotary vane pump. The dry disulfonyl dichloride was dissolved in anhydrous *N,N*-dimethylformamide (30 ml), *N*-(3-aminopropyl)methacrylamide hydrochloride (1.88 mmol, 336 mg) and triethylamine (4.71 mmol, 0.65 ml) were added. After stirring for 3 h at RT, the product was precipitated with 0.1 M aqueous HCl/saturated aqueous NaCl 1:1 (V/V) (200 ml), separated by centrifugation and washed with water (3 * 150 ml). The crude product was purified by column chromatography with silica gel (40 – 63 μ m) as the stationary and CHCl₃:MeOH 97/3 as the mobile phase to yield **4c** (308 mg, 53 %). NMR spectroscopy: δ_{H} (300 MHz, CDCl₃) 8.67 (4 H, s, ArH (Core)), 8.18 (1 H, d, *J* 8.4, ArH), 7.84 (2 H, s, ArH), 7.51 (1 H, d, *J* 8.4, ArH), 6.23 (2 H, q, *J* 6.7, SO₂NH), 5.55-5.80 (4 H, s and br s, C=CH (2 H) and CONH (2 H)), 5.37 (2 H, s, C=CH), 4.20 (1 H, p, *J* 6.2, ArCH), 3.47 (4 H, m, SO₂NCH₂), 3.13 (4 H, br s, CONCH₂), 2.79 (2 H, hex, *J* 6.6, ArCH), 2.63 (1 H, p, *J* 6.5, ArCH), 1.98 (6 H, s, C=CCH₃), 1.74 (4 H, p, *J* 6.9, SONCH₂CH₂CH₂N), 1.20 (24 H, m, ArCHCH₃). MALDI-TOF *m/z* 1255.2783 found, 1255.2802 calculated.

N-3-([*N*-(3-(methacryloylamino)propyl)amino]sulfonyl)-2,6-diisopropylphenyl)-*N'*-(4-([*N*-(3-(methacryloylamino)propyl)amino]sulfonyl)-2,6-diisopropylphenyl)-1-(4-methyl-1-piperazinyl)-6,7,12-trichloroperylene-3,4:9,10-tetracarboxylic bisimide (**3**)



Scheme ESI4: Preparation of **3**.

4b (300 mg, 0.239 mmol) was added to a mixture of *N*-methylpiperazine (2 ml, 18 mmol) and 1-methyl-2-pyrrolidone (3 ml) and stirred 40 °C for 45 min. The crude product was precipitated with 0.1M aqueous HCl/saturated aqueous NaCl 1:1 (V/V) (40 ml), washed with water/saturated aqueous NaHCO₃ 9:1 (V/V) (2 * 40 ml) and water (2 * 40 ml) and purified by column chromatography (silica gel, 40 – 63 μm), eluting with CH₂Cl₂:MeOH 25:1 (V/V), yielding **3** (136 mg, 43 %). NMR spectroscopy: δ_H (300 MHz, CDCl₃) 8.66-8.78 (2 H, m, ArH (Core)), 8.49-8.62 (2 H, m, ArH (Core)), 8.14 (1 H, d, *J* 8.2, ArH), 7.84 (2 H, s, ArH), 7.49 (1 H, d, *J* 8.2, ArH), 6.40 (2 H, br s, SO₂NH), 6.00 (2 H, br s, CONH), 5.75 (2 H, s, C=CH), 5.35 (2 H, s, C=CH), 4.32 (2 H, br s, NCH₂CH₂N), 4.18 (1 H, m, ArCH(1)), 3.30-3.53 (4 H, m, SO₂NCH₂), 2.95-3.20 (5 H, m, CONCH₂ (4 H) and NCH₂CH₂N (1 H)), 1.99-2.95 (11 H, m, NCH₂CH₂N (5 H) and ArCH (3 H) and NCH₃ (3 H)), 1.87-1.99 (6 H, s, C=CCH₃), 1.71 (4 H, m, SONCH₂CH₂CH₂N), 1.19 (24 H, m, ArCHCH₃). MALDI-TOF *m/z* 1319.4100 found, 1319.4034 calculated.

Preparation of pH sensors with covalently linked indicator dye

Microscope slides (76 mm x 26 mm x 1 mm) were functionalised with acrylate groups by covering them with a solution of methacryloxypropylmethyldichlorosilane (0.02 ml) in anhydrous tetrahydrofuran (THF; 1 ml). After incubating for 10 min in an inert atmosphere, the slides were washed with acetone and dried (60 °C, 10 min). A monomer mixture consisting of 1-acryloylmorpholine (95 mg), polyethylenglycol diacrylate (5 mg; average molecular weight 700 g mol⁻¹), photoinitiator 2-hydroxy-4'-(2-hydroxyethoxy)-2-methylpropiophenone (0.05 mg) and indicator dye **3** (0.2 mg) was added onto a functionalised microscope slide in an argon atmosphere and closed up tightly putting another microscope slide on top to yield a 26 mm x 26 mm layer of homogeneously distributed monomer mixture. Illumination with a 366 nm UV light source (4 * 9 W, Jolifin "Tunnel", www.jolifin.com) for 6 min afforded polymer layers which were washed with THF/H₂O 1:1 (V/V) for 30 min prior to use. The layer thickness can be adjusted by attaching spacers of defined thickness onto the microscope slide used for closing up. In this work, the layer thickness of 20 μm was used. For the preparation of dually lifetime referenced sensors, the following cocktail composition was used: 1-acryloylmorpholine (48 mg), polyethylenglycol diacrylate (2 mg), photo-initiator (0.06 mg), dye **3** (0.067 mg), chrome(III)-doped gadolinium aluminium borate (17 mg; composition: GdAl_{2.925}Cr_{0.075}(BO₃)₄).

Preparation of pH sensors with physically entrapped indicator dye

A "cocktail" containing indicator dye **1 - 3** (0.21 mg), hydrogel D4 (41 mg) and EtOH/H₂O 9:1 (V/V) (500 μl) was knife-coated on a dust-free Mylar support to obtain a sensing layer of 7.5 μm thickness after solvent evaporation.

NMR spectroscopy

The structures of **1** and **2** are unequivocally confirmed by ^1H - and ^{13}C -NMR, as well as two-dimensional NMR (HH-COSY and HSQC). The 2D spectra have been included since the 4-methyl-1-piperazinyl and the 4-morpholinyl substituent show relatively broad ^1H -resonances and cause complicated ^1H -spectra. The 2D-methods provide a further proof for the accuracy of the assigned fine structures.

For **3**, limited solubility and the large number of different carbons (67 carbons none of which are fully equivalent) made it impossible to obtain a useful ^{13}C -spectrum. **3** is a mixture of different isomers which differ in the exact substitution pattern of the *N*-aryl substituents after chlorosulfonation, as will be discussed in more detail near figure ESI18. Nevertheless, the following ^1H - and two-dimensional NMR spectra without a doubt confirm that **3** carries two polymerisable groups, while the structure of the perylene bisimide centre is equal to **1** - that is further confirmed by mass spectroscopy as shown in fig. ESI25 and ESI30. The exact substitution pattern of the *N*-aryl group, which essentially acts as a linker between the chromophore centre and the polymerisable groups, is not of major importance to the presented concept.

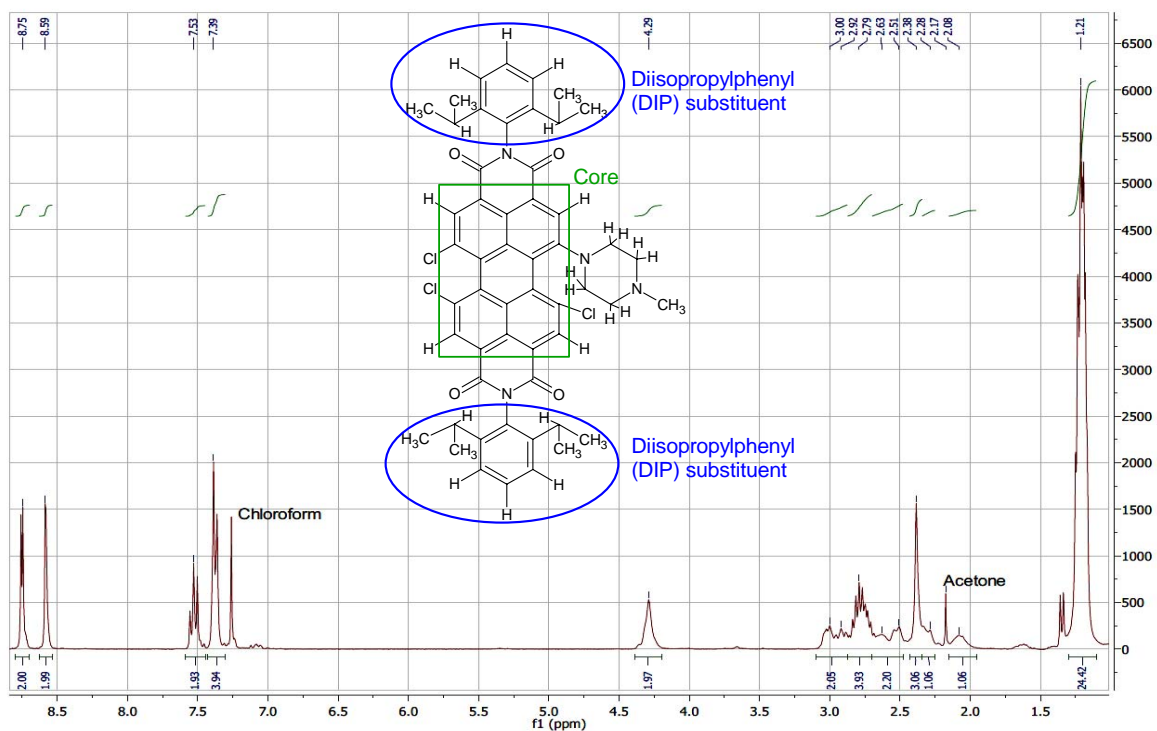


Figure ESI10: $^1\text{H-NMR}$ of **1**: δ_{H} (300 MHz, CDCl_3) 8.75 (2 H, d, ArH (Core)), 8.59 (2 H, d, ArH (Core)), 7.53 (2 H, t, J 7.8, ArH (DIP)), 7.38 (4 H, d, J 7.8, ArH (DIP)); 4.29 (2 H, br s, NCH_2), 2.87-3.10 (2 H, m, NCH_2), 2.70-2.87 (4 H, m, ArCH), 2.48-2.70 (2 H, m, NCH_2), 2.38 (3 H, s, NCH_3), 2.25-2.34 (1 H, br s, NCH_2), 1.96-2.15 (1 H, br s, NCH_2), 1.21 (24 H, m, ArCHCH_3).

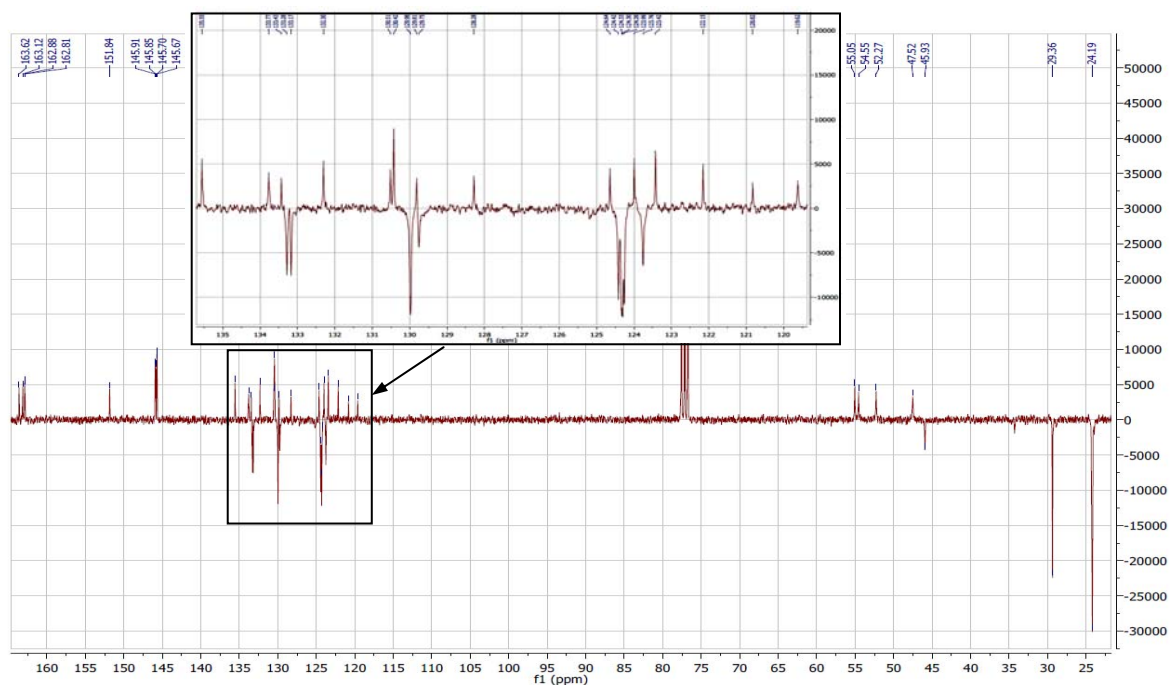


Figure ESI11: $^{13}\text{C-APT-NMR}$ of **1**: δ_{C} (300 MHz, CDCl_3) 163.6, 163.1, 162.9, 162.8 (C=O); 151.8; 145.9 (2 C), 145.7 (2 C), 135.6, 133.8 (2 C), 133.4, 133.3, 133.2, 132.3, 130.5, 130.4, 130.0 (2 C), 129.8, 129.7, 128.3, 124.6, 124.3-124.4 (4 C), 124.0, 123.8, 123.4, 122.1, 120.8, 119.6 (aromatic); 55.1, 54.6, 52.3, 47.5, 45.9 (NCH_2); 29.3-29.5 (multiple C, ArCH); 24.1-24.4 (multiple C, ArCHCH_3). Underlined peaks are of negative intensity (CH or CH_3), those in italics can be found in the HSQC spectrum.

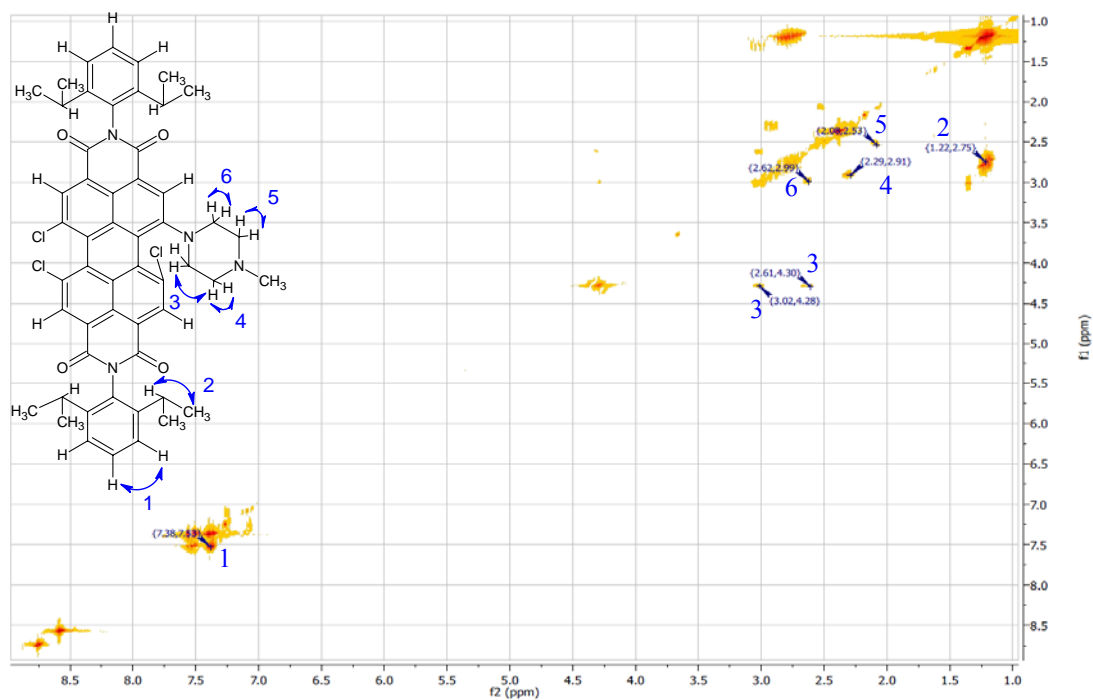


Figure ESI12: HH COSY-NMR of **1** (300 MHz, CDCl₃).

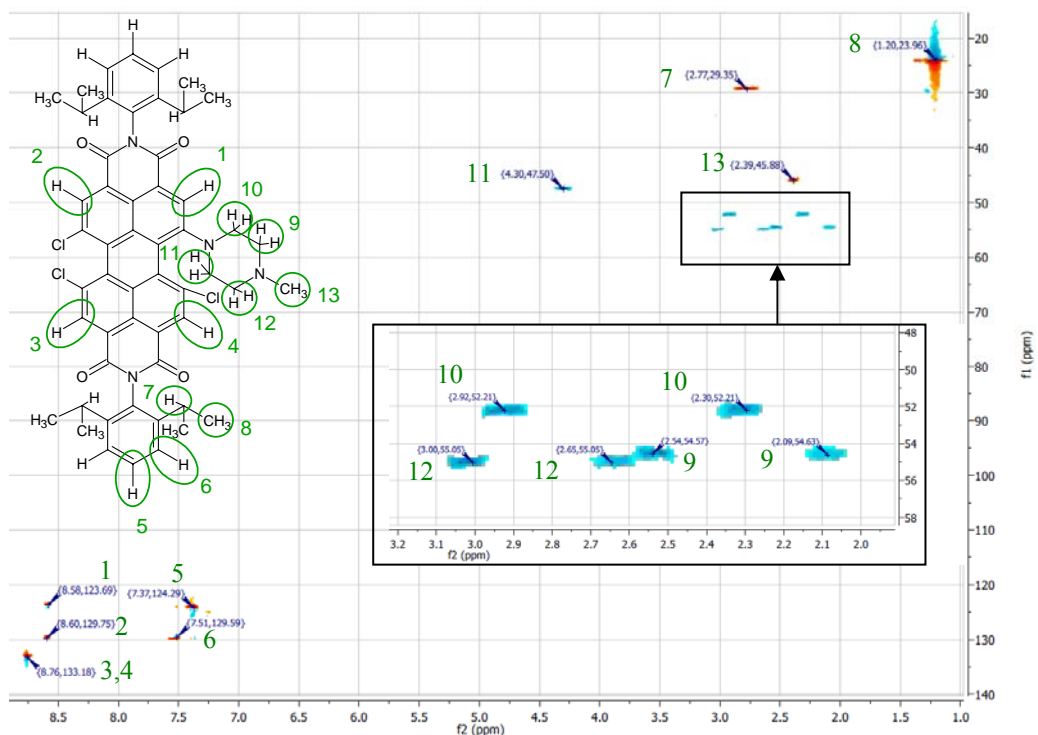


Figure ESI13: HSQC-NMR of **1** (300 MHz, CDCl₃). All unmarked carbons carrying protons are undistinguishable in signal from a marked one due to molecular symmetry.

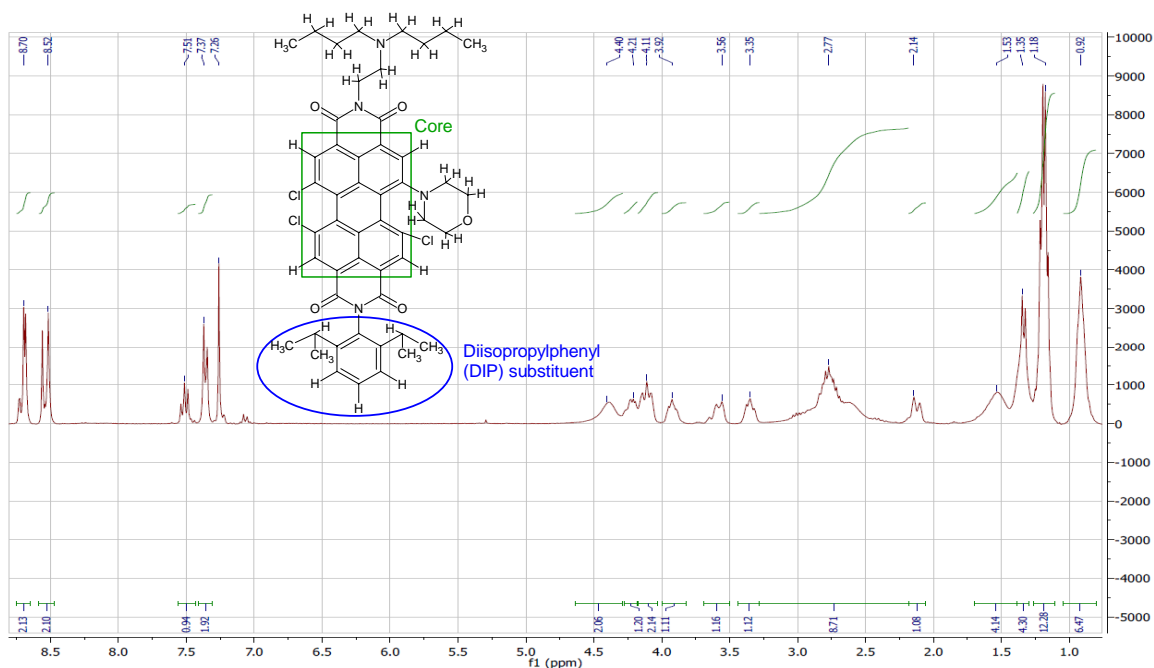


Figure ESI14: $^1\text{H-NMR}$ of **2**: δ_{H} (300 MHz, CDCl_3) 8.70 (2 H, d, ArH (Core)), 8.52 (2 H, d, ArH (Core)), 7.51 (1 H, t, J 7.8, ArH(DIP)), 7.37 (2 H, d, J 7.8, ArH(DIP)), 4.40 (2 H, br s, $(\text{CO})_2\text{NCH}_2$), 4.18-4.28 (1 H, m, $\text{NCH}_2\text{CH}_2\text{O}$), 4.04-4.18 (2 H, m, $\text{NCH}_2\text{CH}_2\text{O}$ (1 H) and OCH_2 (1 H)), 3.82-4.00 (1 H, m, OCH_2), 3.50-3.69 (1 H, m, OCH_2), 3.28-3.43 (1 H, m, OCH_2), 2.18-3.28 (9 H, m, $(\text{CO})_2\text{NCH}_2\text{CH}_2\text{N}$ (2 H) and NCH_2 (4 H) and $\text{NCH}_2\text{CH}_2\text{O}$ (1 H) and ArCH (2 H)), 2.06-2.18 (1 H, m, $\text{NCH}_2\text{CH}_2\text{O}$), 1.38-1.69 (4 H, br s, NCH_2CH_2), 1.30-1.38 (4 H, m, $\text{NCH}_2\text{CH}_2\text{CH}_2$), 1.11-1.27 (12 H, q, J 5.9, ArCHCH $_3$), 0.92 (6 H, t, $\text{NCH}_2\text{CH}_2\text{CH}_2\text{CH}_3$).

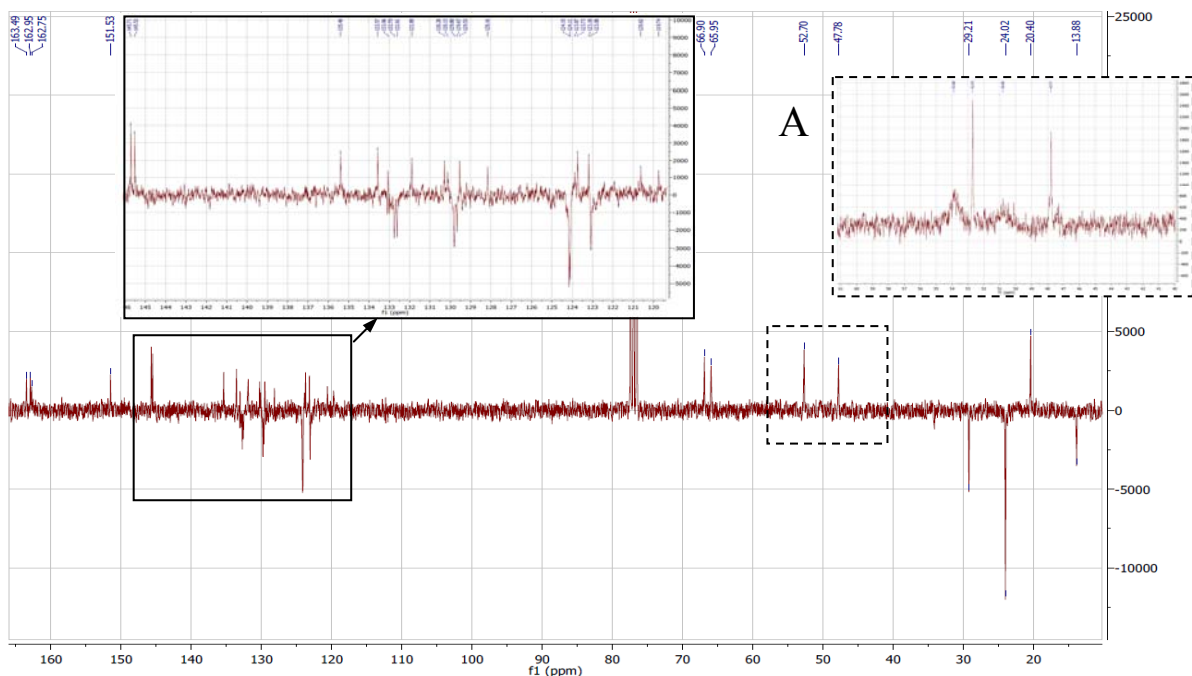


Figure ESI15: $^{13}\text{C-APT-NMR}$ of **2**: δ_{C} (300 MHz, CDCl_3) 163.5, 162.9, 162.7 (2 C) ($\text{C}=\text{O}$); 151.5, 145.7, 145.5, 135.4, 133.6, 133.1, 132.7, 132.6, 131.9, 130.3, 130.1 (2 C), 129.8, 129.7, 129.5, 128.1, 124.2, 124.1, 123.9, 123.7, 123.2, 123.1, 120.6, 119.8 (aromatic); 66.9, 66.0 (OCH_2); 53.9 (*broad*)^A, 52.7, 50.8 (*broad*)^A, 47.8 (NCH_2); 29.2 (ArCH); 24.0 (ArCHCH $_3$); 20.4, 13.9 (Alkyl). Underlined peaks are of negative intensity (CH or CH $_3$), those in italics can be found in the HSQC spectrum. Box **A**: Detail of a standard (not APT) ^{13}C spectrum. The broad peaks cannot be found in the $^{13}\text{C-APT}$ spectrum, however they were found in HSQC (figure ESI13, peaks 14 and 15).

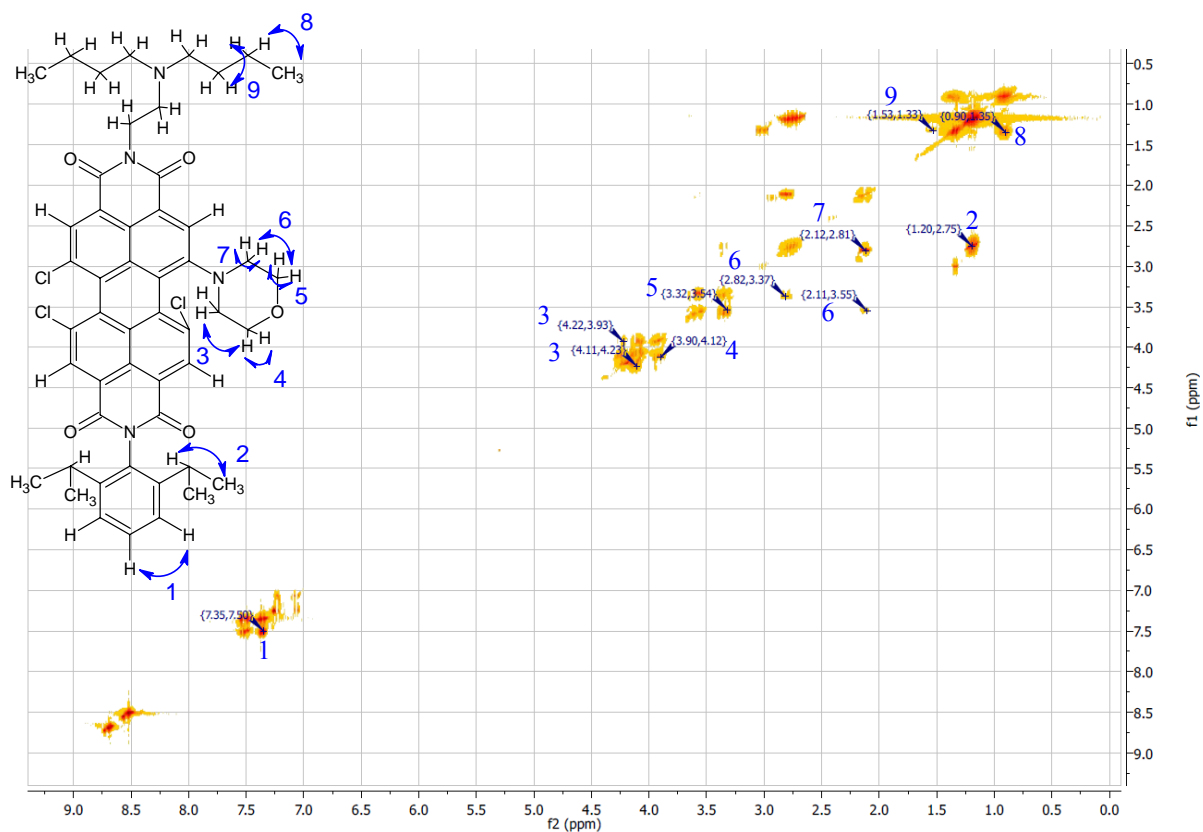


Figure ESI16: HH COSY-NMR of **2** (300 MHz, CDCl₃).

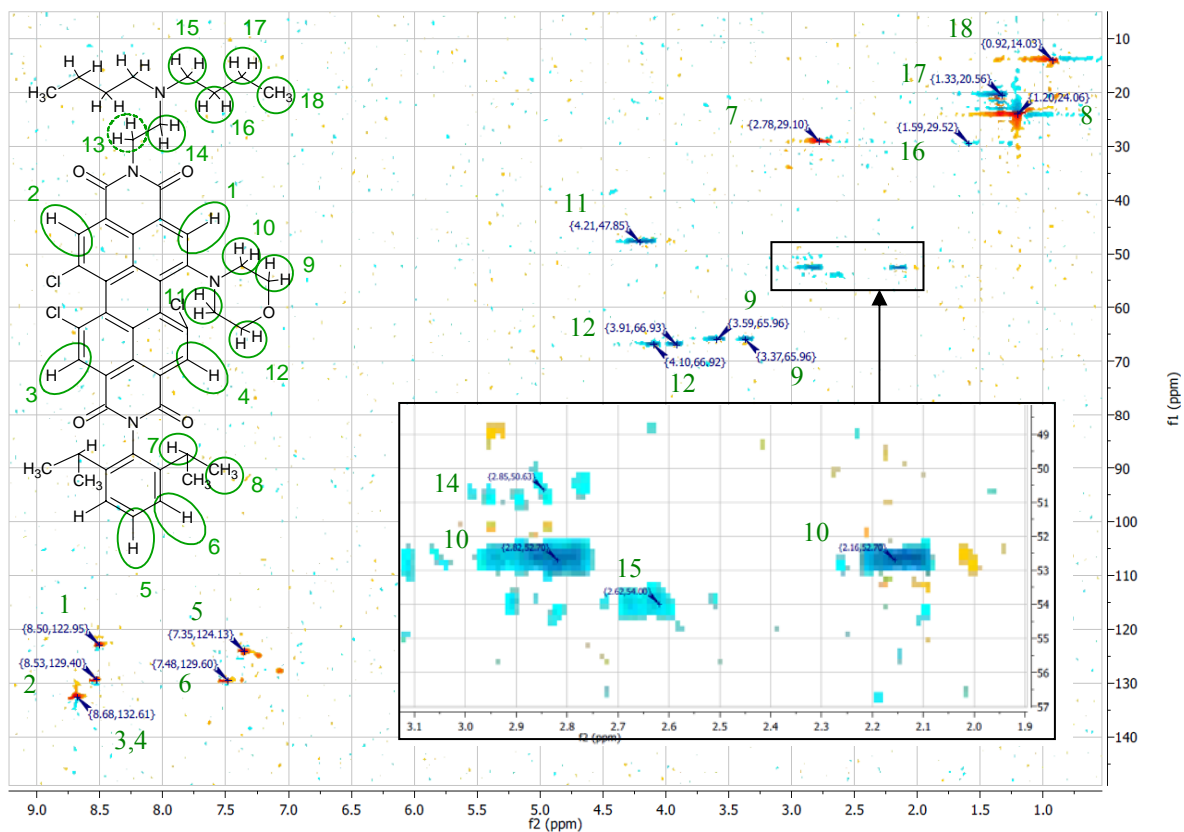


Figure ESI17: HSQC-NMR of **2** (300 MHz, CDCl₃). All unmarked carbons carrying protons are undistinguishable in signal from a marked one due to molecular symmetry.

In dye **3**, NMR spectroscopy reveals that the chlorosulfonation of the 2,6-diisopropylphenyl group can lead to substitution in the 3,5- and in the 4-position. That is expected since steric effects (vicinity of the relatively bulky isopropyl group) here favour 4-substitution while electronic (*o,p*-directing influence of the isopropyl group) and statistic (superior number of positions) effects favour 3,5-substitution. The signals of the unsubstituted group (7.51 ppm, 1 H, t and 7.37 ppm, 2 H, d) have been replaced by signals corresponding to 4-substitution (7.84 ppm, 2 H, s) and to 3,5-substitution (7.49 ppm, 1 H, d and 8.14 ppm, 1 H, d) in an approximate ratio of 1:1 (integral areas). For the sake of clarity, the assumed product structure here carries two differently substituted 2,6-diisopropylphenyl rings. The product may in reality also contain products where both rings are 4-substituted or both are 3,5-substituted. Other signals with low integrals (e.g. those at 7.55-7.75 ppm) are due to other products with even different substitution patterns, since under the acidic conditions of chlorosulfonation the isopropyl groups may migrate to others than the 2,6-positions. However, the exact substitution pattern of the diisopropylphenyl groups is not expected to have any significant impact on the investigated spectral and pH-dependent properties, since they are fully electronically separated from both the chromophore and the piperazinyl (pH receptor) moieties. MALDI-TOF mass spectroscopy (fig. ESI25) and LCMS (fig. ESI30) confirm that **3** contains only the isomers.

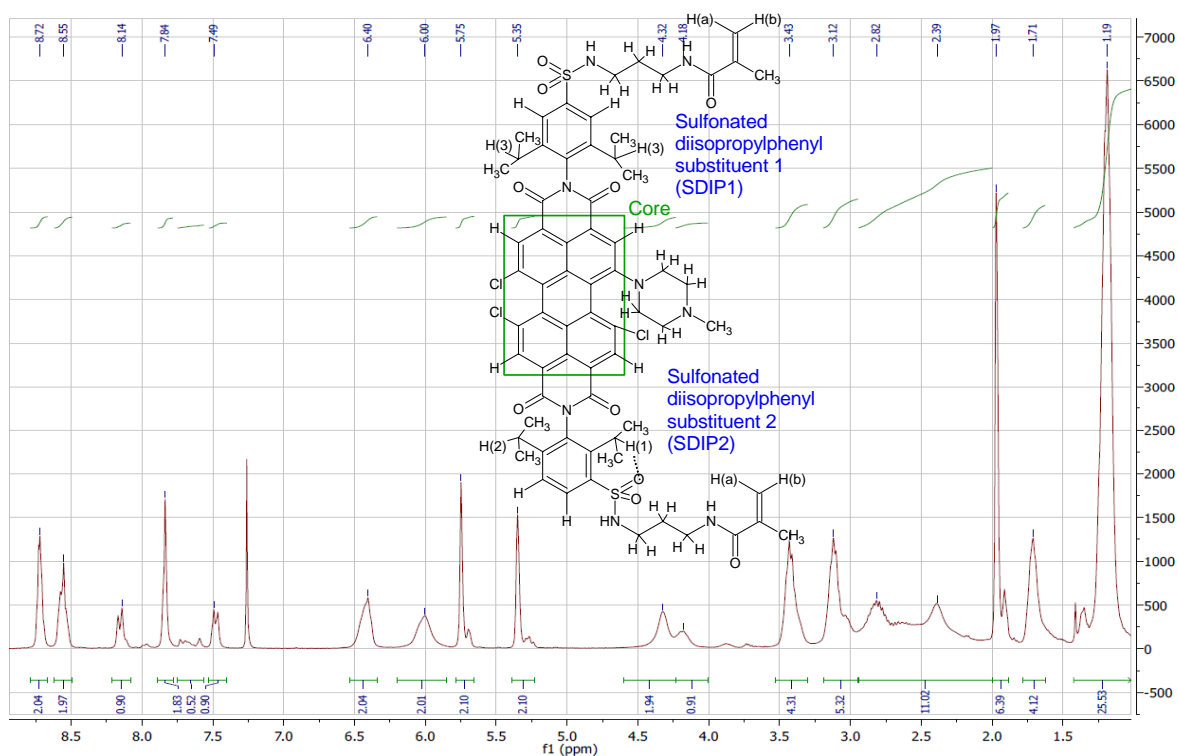


Figure ESI18: $^1\text{H-NMR}$ of **3**: δ_{H} (300 MHz, CDCl_3) 8.66-8.78 (2 H, m, ArH (Core)), 8.49-8.62 (2 H, m, ArH (Core)), 8.14 (1 H, d, J 8.2, ArH(SDIP2)), 7.84 (2 H, s, ArH(SDIP1)), 7.49 (1 H, d, J 8.2, ArH(SDIP2)), 6.40 (2 H, br s, SO_2NH), 6.00 (2 H, br s, CONH), 5.75 (2 H, s, $\text{C}=\text{CH}(\text{a})$), 5.35 (2 H, s, $\text{C}=\text{CH}(\text{b})$), 4.32 (2 H, br s, $\text{NCH}_2\text{CH}_2\text{N}$), 4.18 (1 H, m, ArCH(1)), 3.30-3.53 (4 H, m, SO_2NCH_2), 2.95-3.20 (5 H, m, CONCH_2 (4 H) and $\text{NCH}_2\text{CH}_2\text{N}$ (1 H)), 1.99-2.95 (11 H, m, $\text{NCH}_2\text{CH}_2\text{N}$ (5 H) and ArCH (3 H) and NCH_3 (3 H)), 1.87-1.99 (6 H, s, $\text{C}=\text{CCH}_3$), 1.71 (4 H, m, $\text{SONCH}_2\text{CH}_2\text{CH}_2\text{N}$), 1.19 (24 H, m, ArCHCH_3).

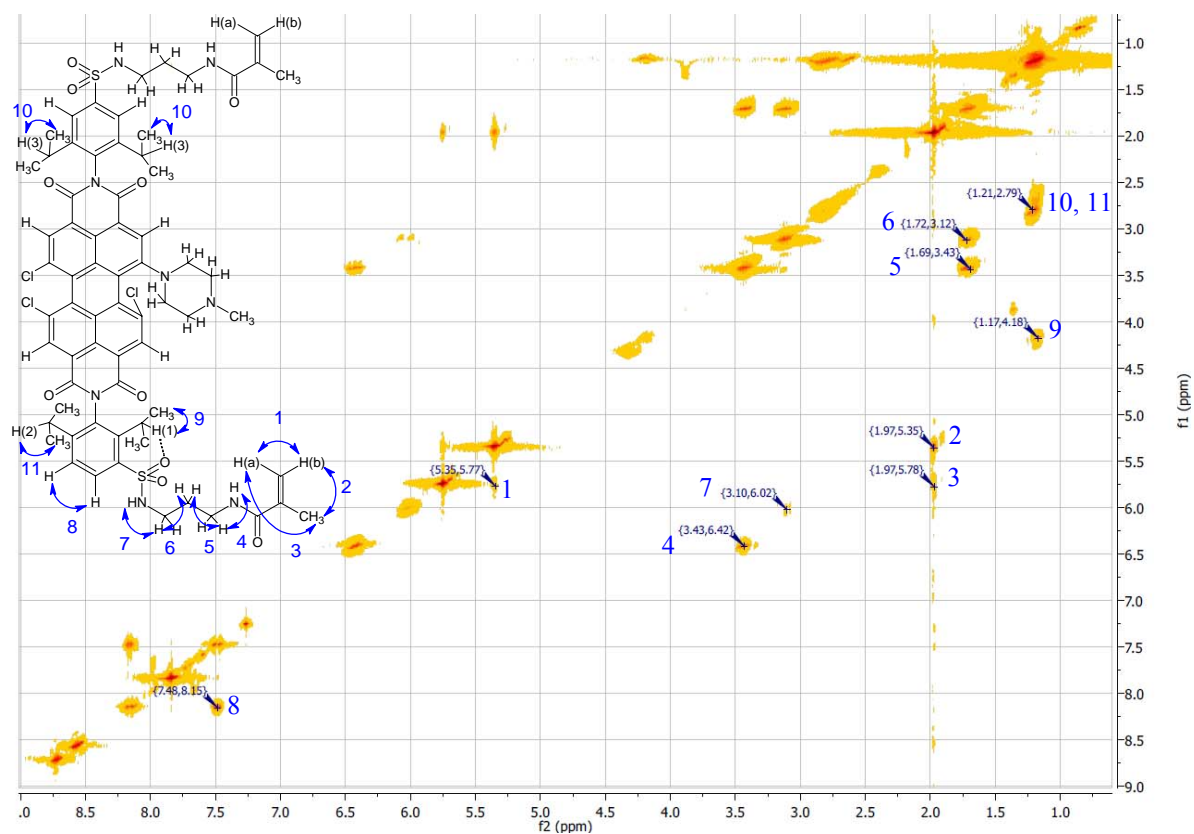


Figure ESI19: HH COSY NMR of **3** (300 MHz, CDCl₃).

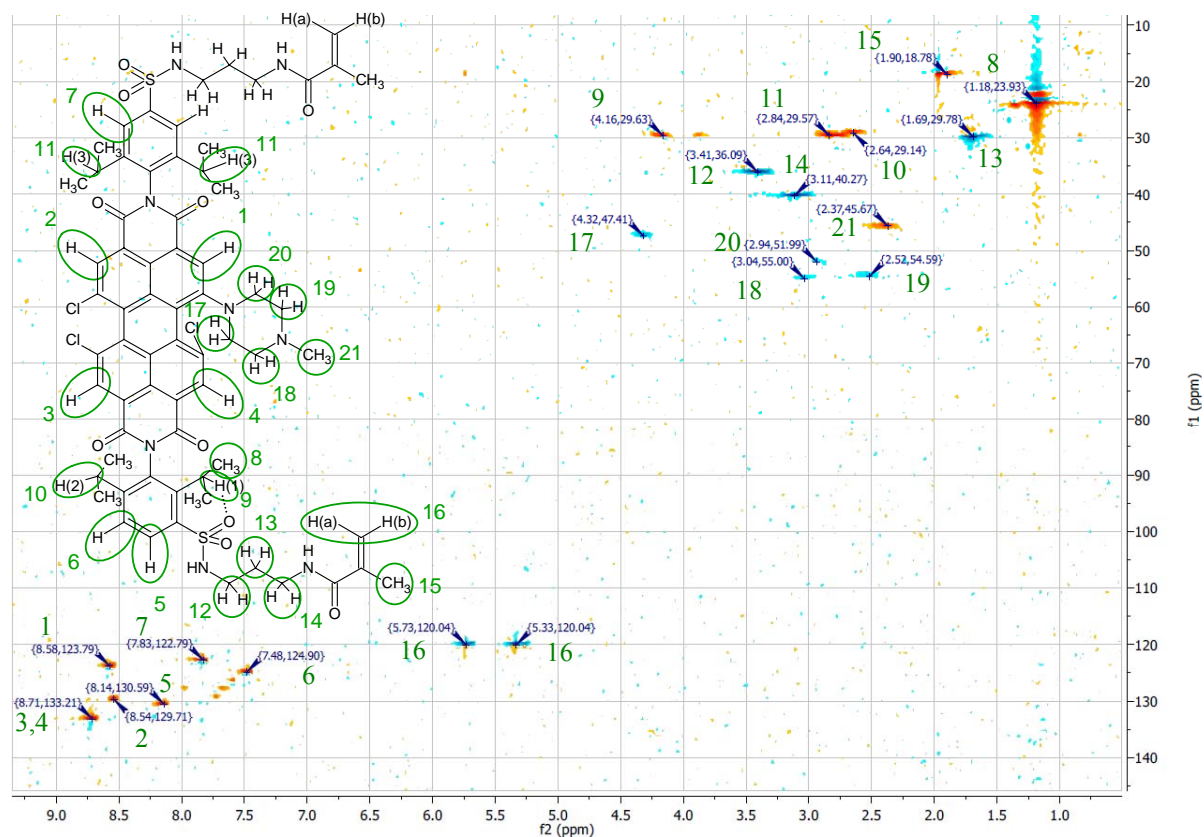


Figure ESI20: HSQC NMR of **3** (300 MHz, CDCl₃). All unmarked carbons carrying protons are undistinguishable in signal from a marked one due to molecular symmetry.

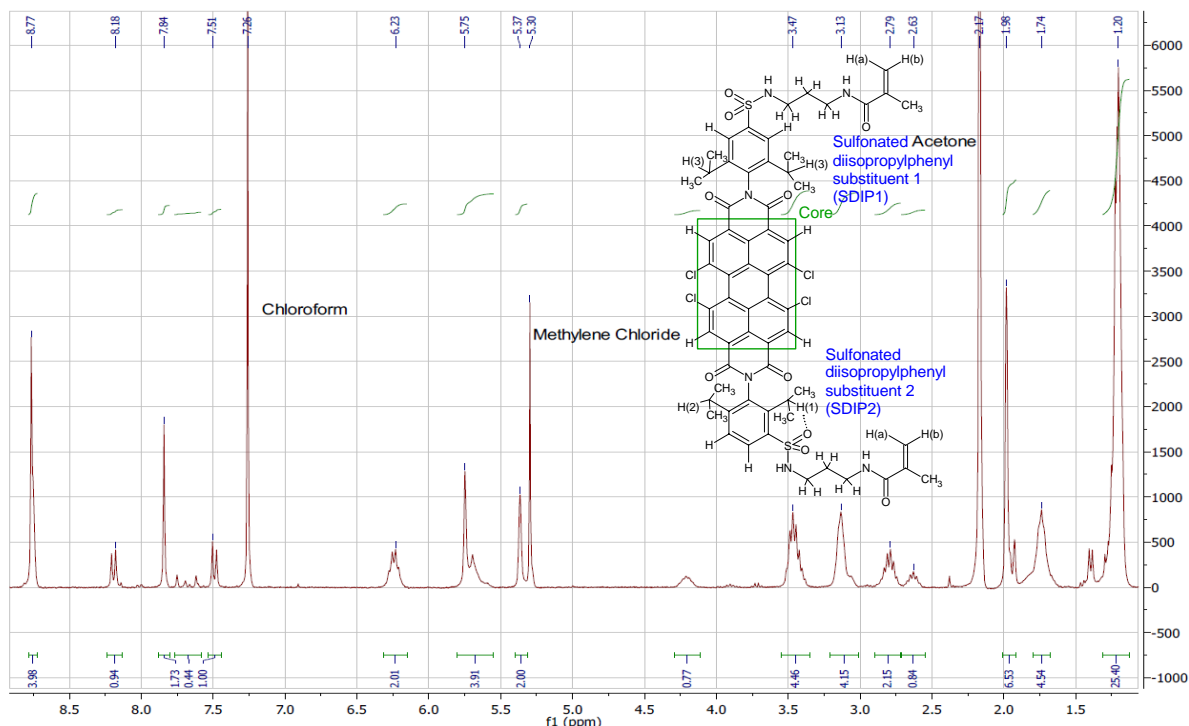


Figure ESI21: $^1\text{H-NMR}$ of **4b**: δ_{H} (300 MHz, CDCl_3) 8.67 (4 H, s, ArH (Core)), 8.18 (1 H, d, J 8.4, ArH(SDIP2)), 7.84 (2 H, s, ArH(SDIP1)), 7.51 (1 H, d, J 8.4, ArH(SDIP2)), 6.23 (2 H, q, J 6.7, SO_2NH), 5.55-5.80 (4 H, s and br s, $\text{C}=\text{CH}(\text{a})$ (2 H) and CONH (2 H)), 5.37 (2 H, s, $\text{C}=\text{CH}(\text{b})$), 4.20 (1 H, p, J 6.2, ArCH(1)), 3.47 (4 H, m, SO_2NCH_2), 3.13 (4 H, br s, CONCH_2), 2.79 (2 H, hex, J 6.6, ArCH(3)), 2.63 (1 H, p, J 6.5, ArCH(2)), 1.98 (6 H, s, $\text{C}=\text{CCH}_3$), 1.74 (4 H, p, J 6.9, $\text{SONCH}_2\text{CH}_2\text{CH}_2\text{N}$), 1.20 (24 H, m, ArCH CH_3).

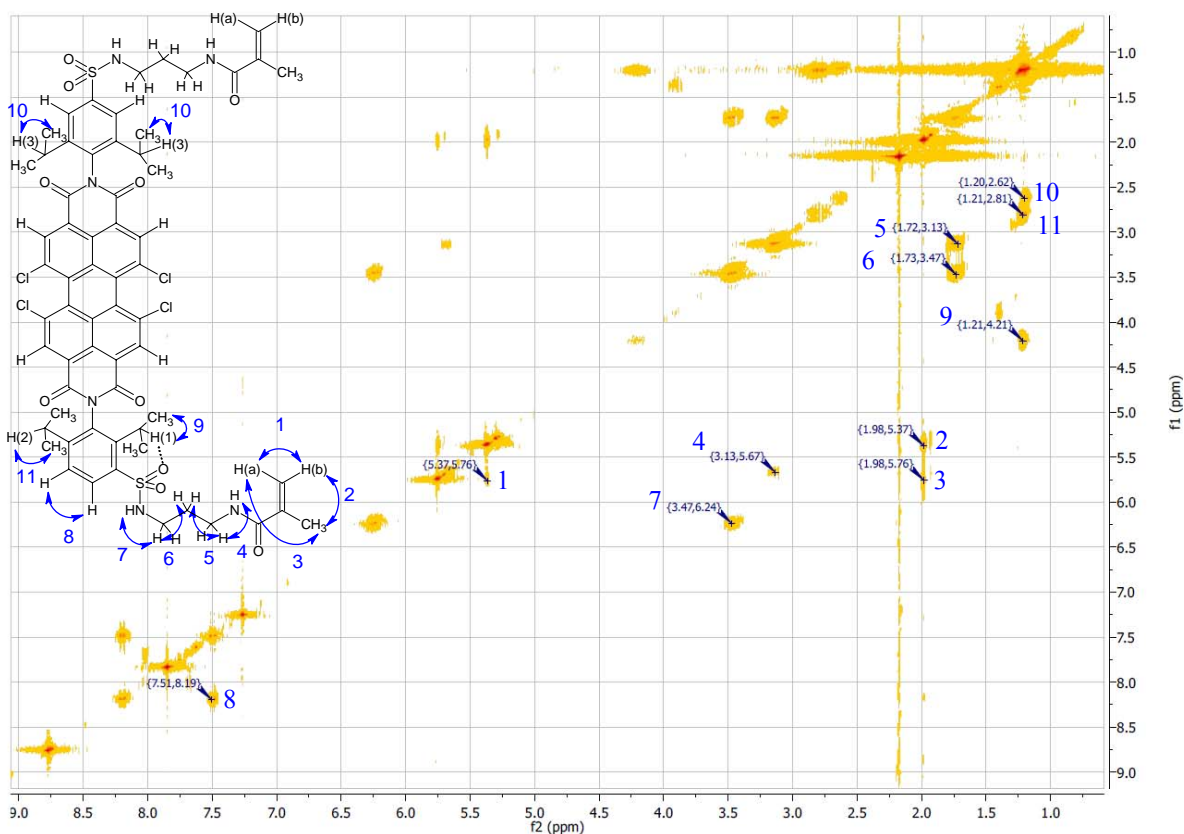


Figure ESI22: HH COSY NMR of **4b** (300 MHz, CDCl_3).

MALDI-TOF mass spectrometry

MALDI-TOF mass spectrometry clearly shows exact masses that are in agreement with the product structures. Other signals, which correspond to $[M-HCl]^+$ and $[M-HCl-2H]^+$, are formed upon MALDI (possibly by a photoreaction) and are not present in the products in significant amounts. That is confirmed by several facts - their formation is strongly enhanced if the laser energy used in MALDI is increased (fig. ESI27); NMR do not show a significant contamination with dechlorinated products (would require further signals in the aromatic range); if electrospray ionisation is employed (fig. ESI28-30), only product masses but no $[M-HCl]^+$ nor $[M-HCl-2H]^+$ are detected.

Dye 1

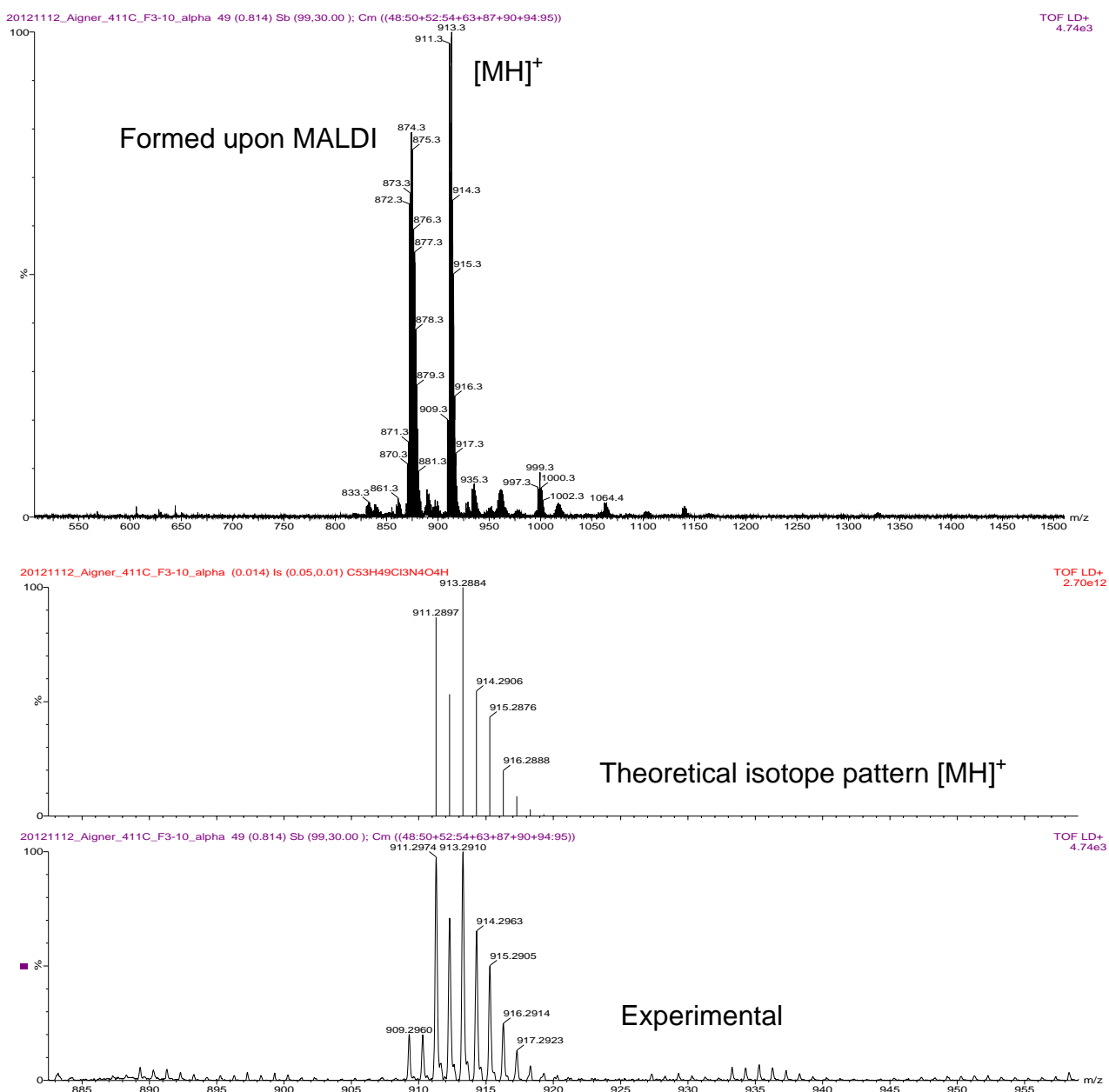


Figure ESI23: MALDI-TOF spectrum of **1**.

Dye 2

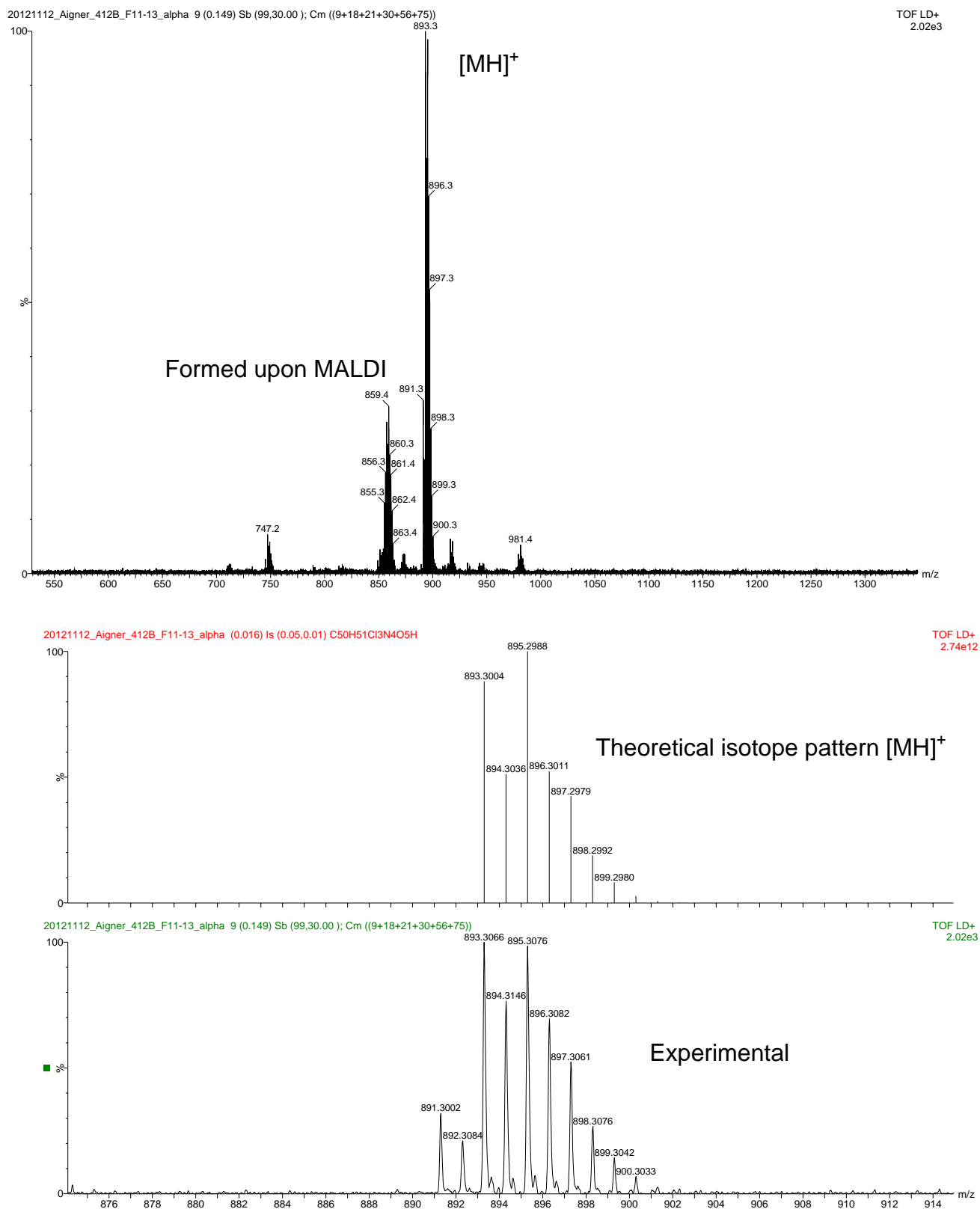


Figure ESI24: MALDI-TOF spectrum of **2**.

Dye 3

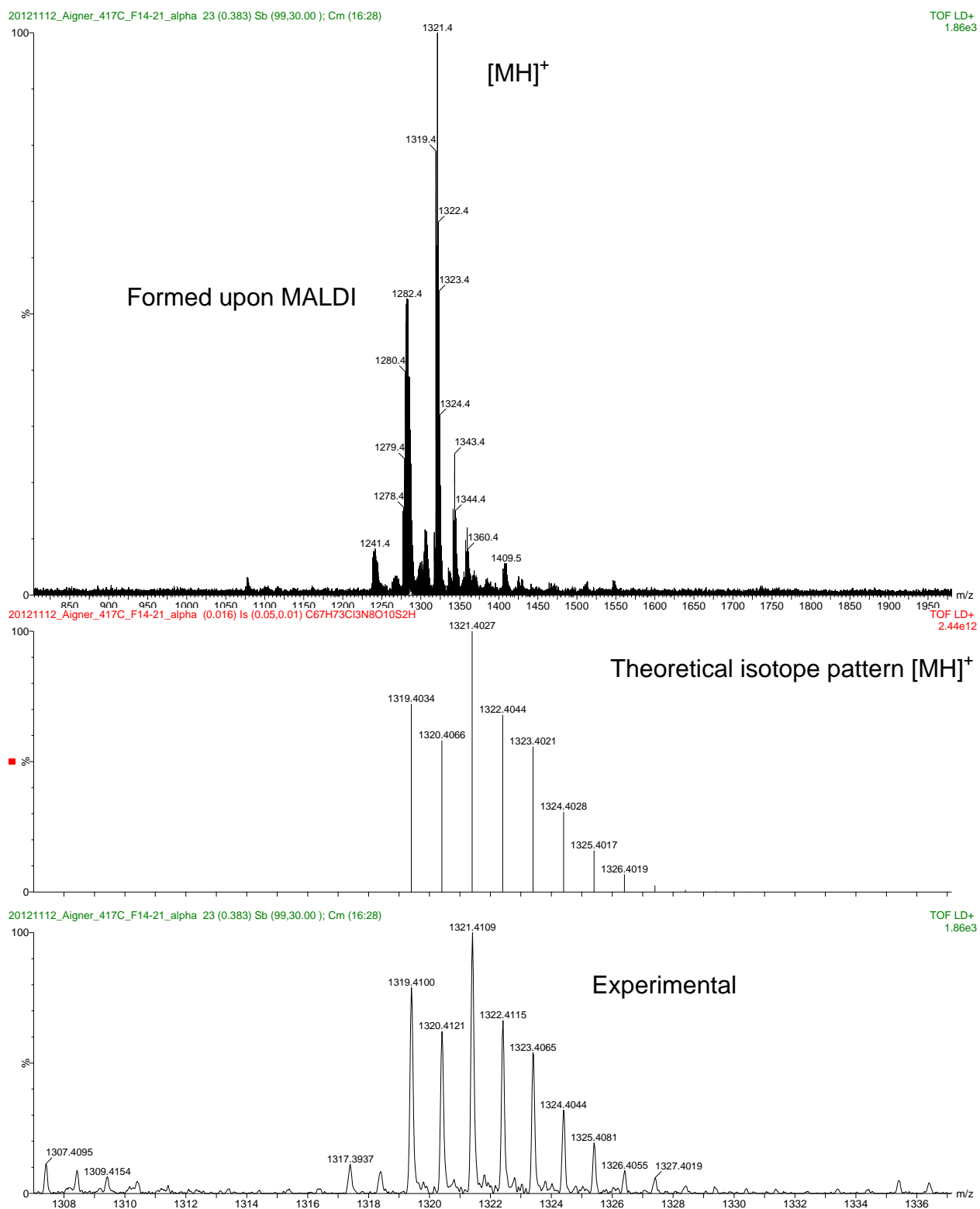


Figure ESI25: MALDI-TOF spectrum of **3**.

Dye 4b

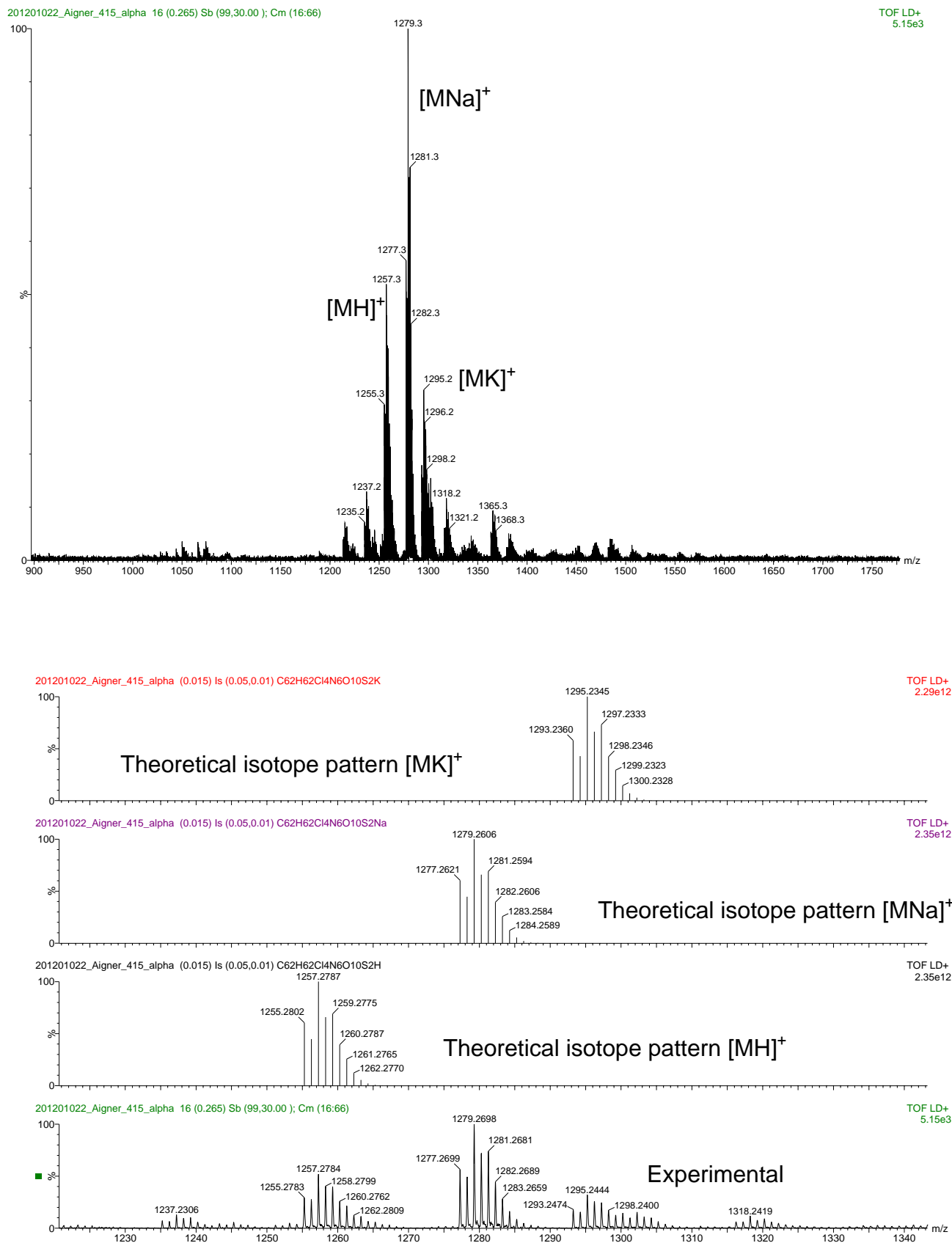


Figure ESI26: MALDI-TOF spectrum of 4c.

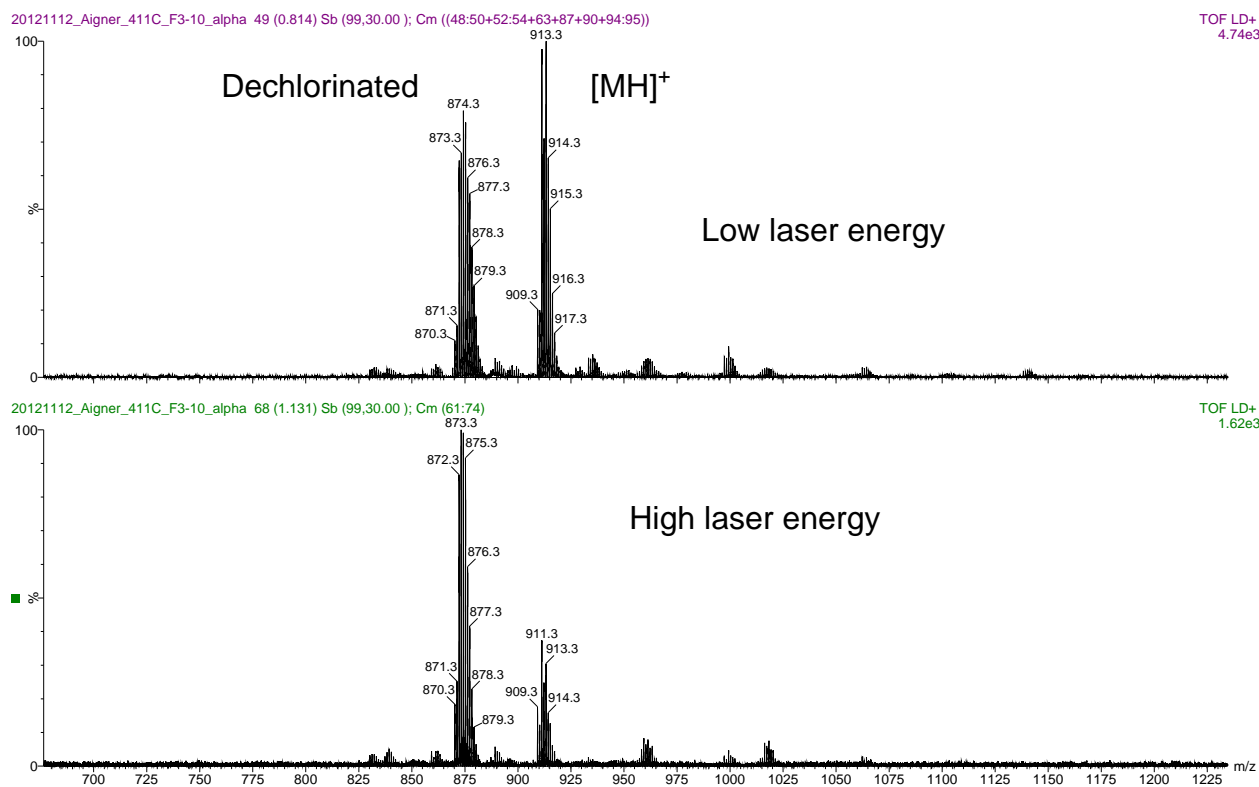


Figure ESI27: MALDI-TOF spectra of **1**, acquired applying different laser energies. The formation of the dechlorinated product is significantly enhanced when higher laser energies are applied, which points out that it could be formed by a photoreaction upon MALDI.

LCMS measurements

In the following LCMS (electrospray ionisation) measurements, the shown mass spectra are fully representative for the whole measurement. No other masses were detected at any time. All chromatograms were measured with a diode array detector set to 640 nm (reference 360 nm subtracted). Gradients are stated in tables ESI1 and ESI2, following fig. ESI30.

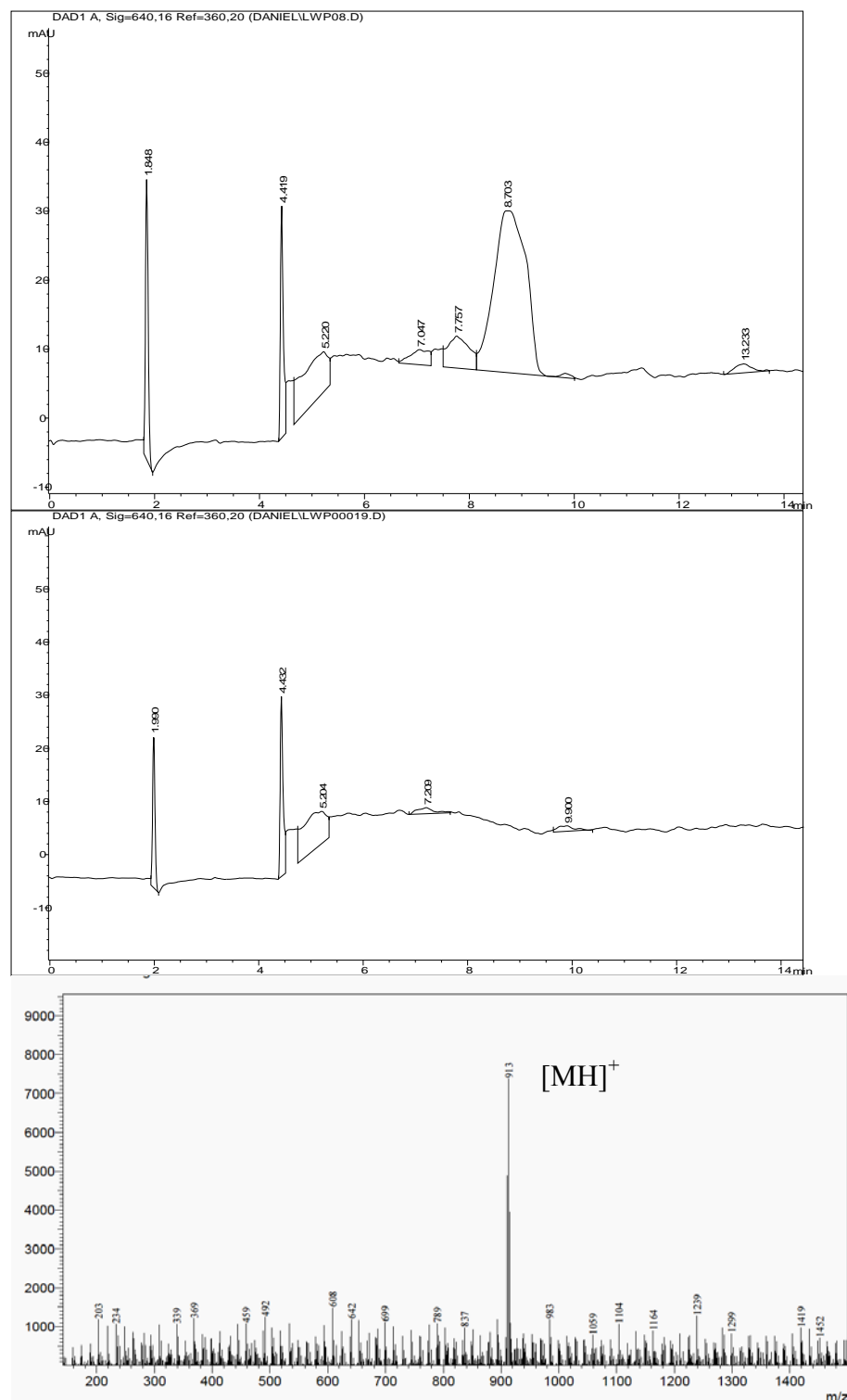


Figure ESI28: HPLC-chromatogram of **1** (top), blank run under the same settings (middle) and mass spectrum obtained by electrospray ionisation (bottom).

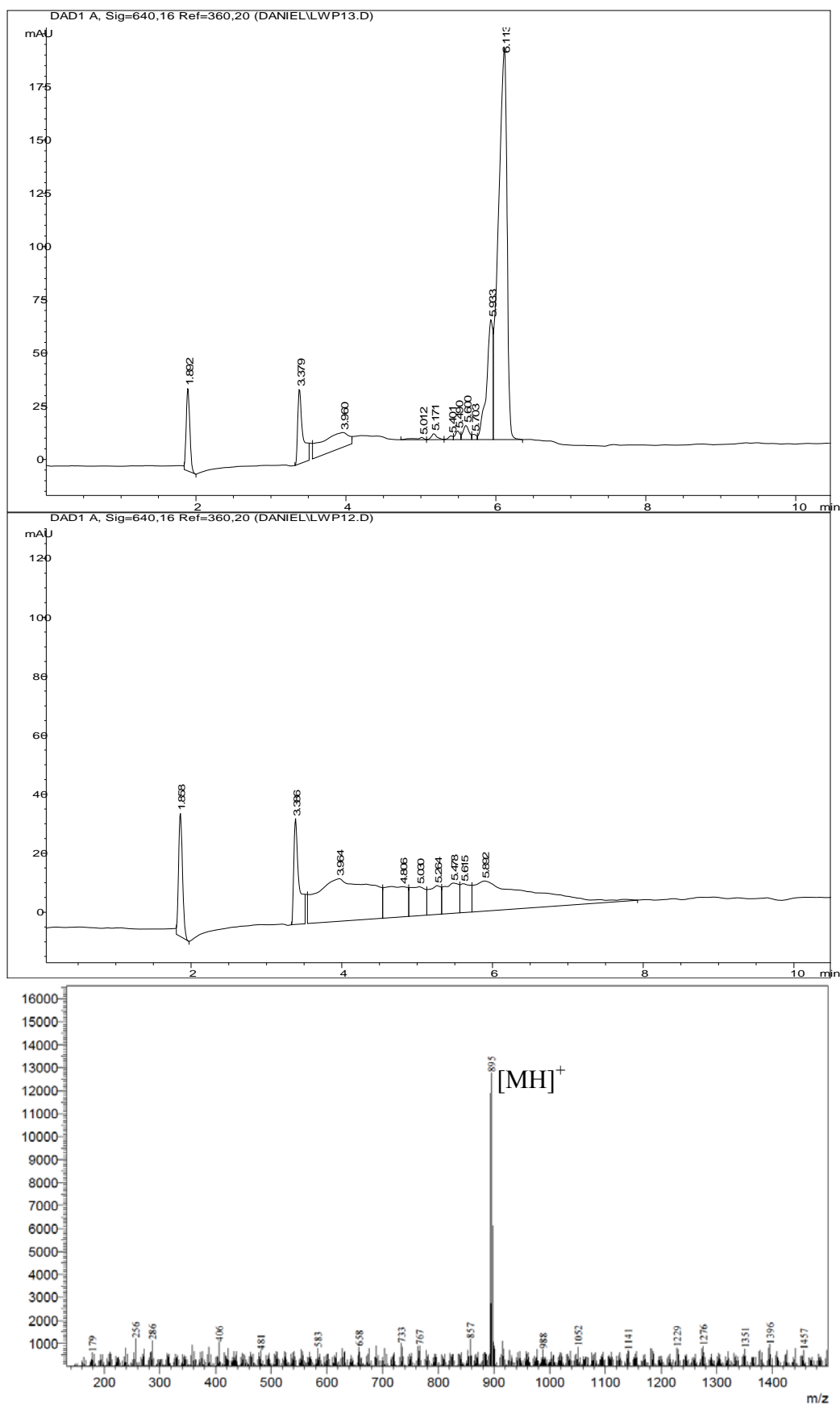


Figure ESI29: HPLC-chromatogram of **2** (top), blank run under the same settings (middle) and mass spectrum obtained by electrospray ionisation (bottom).

As discussed earlier, **3** is an isomeric mixture due to different substitution pattern formed upon chlorosulfonation. Note that no other masses than $[MNa]^+$ were detected in the whole sample.

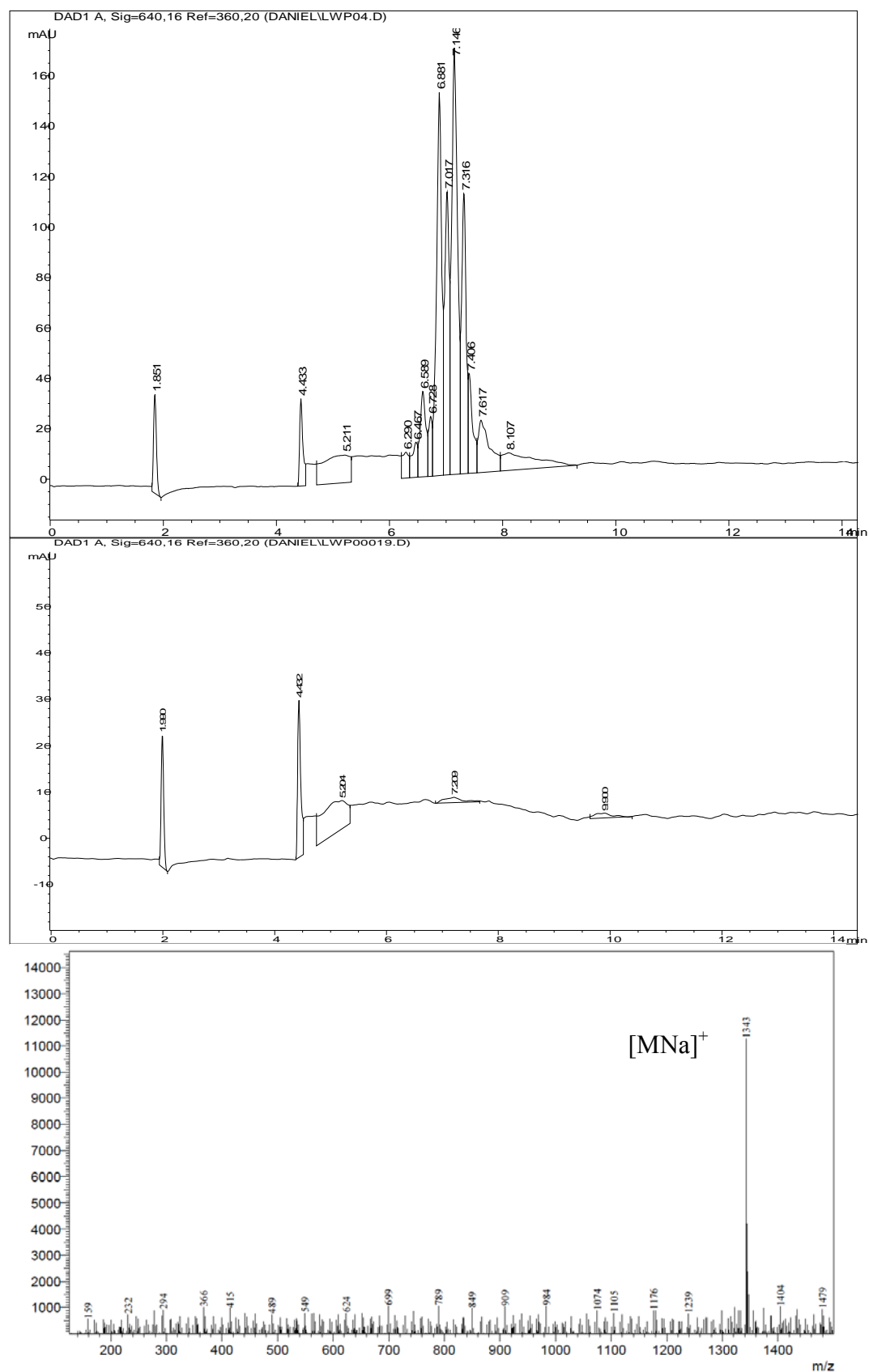


Figure ESI30: HPLC-chromatogram of **3** (top), blank run under the same settings (middle) and mass spectrum obtained by electrospray ionisation (bottom).

Table ESI1: Elution gradient used for LCMS characterisation of **1** and **2**

Time/min	Ratio CH ₃ CN/%	Ratio 0.1% aqueous HOAc/%	Flow rate/ml·min ⁻¹
0	0	100	1
5	100	0	1
10	100	0	1
11	0	100	1
15	0	100	1

Table ESI2: Elution gradient used for LCMS characterisation of **3**

Time/min	Ratio CH ₃ CN/%	Ratio 0.1% aqueous HOAc/%	Flow rate/ml·min ⁻¹
0	0	100	1
1	40	60	1
8	75	25	1
9	100	0	1
11	100	0	1
12	0	100	1
16	0	100	1

References

1. D. Aigner, S. M. Borisov, and I. Klimant, *Anal Bioanal Chem*, 2011, **400**, 2475–2485.
2. S. M. Borisov, K. Gatterer, B. Bitschnau, and I. Klimant, *J. Phys. Chem. C*, 2010, **114**, 9118–9124.
3. R. Sens and K. H. Drexhage, *Journal of Luminescence*, 1981, **24–25, Part 2**, 709–712.